

Improving statistical power in severe malaria genetic association studies by augmenting phenotypic precision

James A Watson^{1,2,†,*}, Carlyne M Ndila^{3,†}, Sophie Uyoga³, Alexander W Macharia³, Gideon Nyutu³, Mohammed Shebe³, Caroline Ngetsa³, Neema Mturi³, Norbert Peshu³, Benjamin Tsofa³, Kirk Rockett^{4,5}, Stije Leopold^{1,2}, Hugh Kingston^{1,2}, Elizabeth C George⁶, Kathryn Maitland^{3,7}, Nicholas P Day^{1,2}, Arjen Dondorp^{1,2}, Philip Bejon^{2,3}, Thomas N Williams^{3,7,‡}, Chris C Holmes^{8,9,‡}, Nicholas J White^{1,2,‡}

1: Mahidol Oxford Tropical Medicine Research Unit, Faculty of Tropical Medicine, Mahidol University, Bangkok, Thailand

2: Centre for Tropical Medicine and Global Health, Nuffield Department of Medicine, University of Oxford, United Kingdom

3: KEMRI-Wellcome Trust Research Programme, Centre for Geographic Medicine Research-Coast, Kilifi 80108, Kenya

4: The Wellcome Trust Sanger Institute, Cambridge, United Kingdom

5: Wellcome Trust Centre for Human Genetics, University of Oxford, Oxford, United Kingdom

6: Medical Research Council Clinical Trials Unit, University College London, United Kingdom

7: Institute of Global Health Innovation, Imperial College, London, United Kingdom

8: Nuffield Department of Medicine, University of Oxford, United Kingdom

9: Department of Statistics, University of Oxford, United Kingdom

†: Joint first authors

‡: Joint senior authors

*Correspondence: jwatowatson@gmail.com

Abstract

Severe falciparum malaria has substantially affected human evolution. Genetic association studies of patients with clinically defined severe malaria and matched population controls have helped characterise human genetic susceptibility to severe malaria, but phenotypic imprecision compromises discovered associations. In areas of high malaria transmission the diagnosis of severe malaria in young children and, in particular, the distinction from bacterial sepsis, is imprecise. We developed a probabilistic diagnostic model of severe malaria using platelet and white count data. Under this model we re-analysed clinical and genetic data from 2,220 Kenyan children with clinically defined severe malaria and 3,940 population controls, adjusting for phenotype mis-labelling. Our model, validated by the distribution of sickle trait, estimated that approximately one third of cases did not have severe malaria. We propose a data-tilting approach for case-control studies with phenotype mis-labelling and show that this reduces false discovery rates and improves statistical power in genome-wide association studies.

1 Introduction

2 Severe malaria caused by the parasite *Plasmodium falciparum* kills nearly half a million children
3 each year, mostly in sub-Saharan Africa [1]. By causing death in children before reaching their
4 reproductive age, *P. falciparum* has exerted a substantial selective evolutionary pressure on the
5 human genome [2, 3]. Recent advances in whole genome sequencing and haplotype imputation
6 [4], combined with data gathered prospectively from large patient cohorts has improved our un-
7 derstanding of genetic susceptibility to *P. falciparum* infection and severe disease [5, 6, 7, 8] but
8 many questions remain unanswered [3]. A major limitation of genetic association studies in se-
9 vere malaria is that the diagnosis of severe falciparum malaria in children is imprecise [9, 10, 11].
10 This imprecision increases with transmission intensity due to the low positive predictive value of

11 blood-stage parasitaemia in areas where the background prevalence of microscopy detectable par-
12 asitaemia in apparently healthy young children is high (typically around 30% [12] but can exceed
13 90%[13]).

14 Severe falciparum malaria has been defined by experts convened by the World Health Orga-
15 nization (WHO) as clinical or laboratory evidence of vital organ dysfunction in the presence of
16 circulating asexual *P. falciparum* parasitaemia [14]. The WHO definition of severe malaria is aimed
17 primarily at clinicians and health care workers managing patients with malaria who appear severely
18 ill. This appropriately prioritises sensitivity over specificity [15]. An inclusive clinical definition
19 ensures that cases are not missed and patients receive the best treatment. In contrast genetic
20 association studies require high specificity [16]. For a given sample size, their statistical power,
21 false-discovery rates and the validity of their interpretation are weakened by phenotypic inaccu-
22 racy. Specificity in the severe malaria diagnosis depends on the prevalence of malaria parasitaemia
23 which reflects background transmission intensity. In areas of low or seasonal transmission (e.g.
24 most of endemic Asia and the Americas), clinical and laboratory signs of severity accompanied by
25 a positive blood film for *P. falciparum* are highly specific for severe malaria, which predominantly
26 affects young adults. In contrast in high transmission areas in sub-Saharan Africa and the islands of
27 New Guinea, where severe malaria is largely a disease of young children, the diagnostic criteria for
28 defining severe malaria are less specific because of the high background prevalence of asymptomatic
29 parasitaemia and the lower specificity of the clinical manifestations. Standard case definitions of
30 severe malaria will therefore inevitably include both patients with non-malarial severe illness with
31 concomitant parasitaemia, and with concomitant non-severe malaria.

32 We developed a probabilistic diagnostic model of severe malaria based on haematological
33 biomarkers using data from 1,704 adults and children mainly from low transmission settings whose
34 diagnosis of severe malaria is considered to be highly specific. We used this model to demonstrate
35 low phenotypic specificity in a cohort of 2,220 Kenyan children who were diagnosed clinically with
36 severe malaria. We validated the predictions using a natural experiment, the distribution of sickle
37 cell trait (HbAS), the genetic polymorphism with the strongest known protective effect against all
38 forms of clinical malaria [6]. Building on work on ‘data-tilting’ [17], we suggest a new method for
39 testing genetic associations in the context of case-control studies in which cases are re-weighted by
40 the probability that the severe malaria diagnosis is correct under the model. As proof-of-concept,
41 we ran a genome-wide association study across 9.6 million bi-allelic variants using the subset of
42 cases with whole-genome sequencing data ($n = 1,297$) and population controls ($n = 1,614$). Ad-
43 justing for case mis-classification decreased genome-wide false-discovery rates [18], and increased
44 effect sizes in the top three regions of the human genome most strongly associated with protection
45 from severe malaria in East Africa (*HBB*, *ABO*, and *FREM3* [7]). A re-analysis of 120 directly
46 typed polymorphisms in 70 candidate malaria-protective genes in the 2,220 Kenyan cases and 3,940
47 population controls, examining differential effects between correctly and incorrectly classified cases,
48 suggests that the protective effect of glucose-6-phosphate dehydrogenase (G6PD) deficiency has
49 been obscured in this population by case mis-classification. Our results show that adding full blood
50 count meta-data - routinely measured in most hospitals in sub-Saharan Africa - to severe malaria
51 cohorts would lead to more accurate quantitative analyses in case-control studies and increased
52 statistical power.

53 Results

54 Reference model of severe malaria

55 We used the joint distribution of platelet counts and white blood cell counts (both on a logarithmic
56 scale) to develop a simple biomarker-based reference model of severe malaria. To fit the reference
57 model (i.e. $P[\text{Data} \mid \text{Severe malaria}]$), we used (i) platelet and white count data from severe
58 malaria patient cohorts enrolled in low transmission areas where severe disease accompanied by
59 a positive blood stage parasitaemia has a high positive predictive value for severe malaria (930
60 adults from Vietnam [19, 20] and 653 adults and children from Thailand and Bangladesh); and (ii)
61 data from severely ill African children with plasma *PfHRP2* concentrations $> 1,000$ ng/ml and $>$
62 $1,000$ parasites per μL of blood (121 children from Uganda [21]). Severe illness accompanied by
63 a high plasma *PfHRP2* concentration makes the diagnosis of severe malaria highly specific [22].
64 The joint distribution of platelet and white blood cell counts in severe malaria was modelled as a
65 bivariate t -distribution with both blood count variables on the \log_{10} scale.

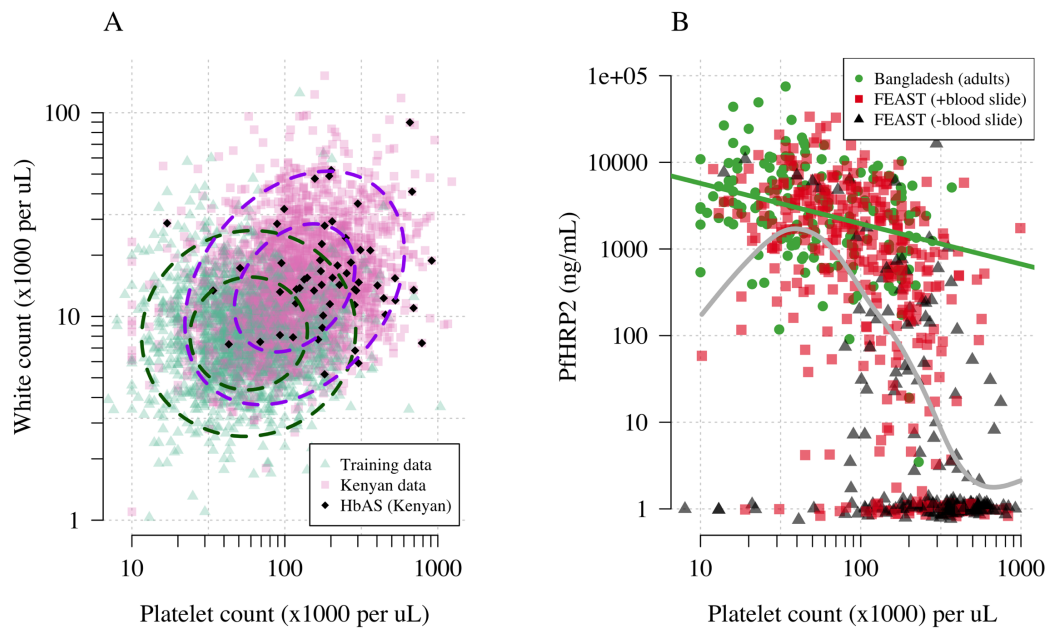


Figure 1: **Platelet counts and white blood cell counts as diagnostic predictors of severe malaria.** Panel A shows the bi-variate marginal distribution in the training data (thought to be highly specific to severe malaria, green triangles, $n = 1,704$) and in the Kenyan case data (pink squares, $n = 2,220$; black diamonds: HbAS). The dashed ellipses show the 50 and 95% bivariate normal probability contours approximating each dataset (dark green: training data; purple: Kenyan data). Panel B shows the relationship between platelet counts and plasma *PfHRP2* in adults and children with severe malaria from Bangladesh (green circles, $n = 172$, the green line shows a linear fit) and in the FEAST trial ($n = 566$, not specific to severe malaria) [21]. Red squares: malaria-positive blood slide; black triangles: malaria-negative blood slide. The grey line shows a spline fit to the FEAST data (*smooth.spline* function in R with default parameters). Undetectable plasma *PfHRP2* concentrations were set to $1 \text{ ng/mL} \pm \text{random jitter}$.

66 Figure 1A shows the training data (green triangles: patients with a highly specific diagnosis of
67 severe malaria) alongside data from a large Kenyan cohort of hospitalised children diagnosed with
68 severe malaria, whose diagnosis had unknown specificity (pink squares). The median platelet count
69 in the training data was 57,000 per μL and the median total white blood cell count was 8,400 per μL .
70 In contrast, the median platelet count in the Kenyan children was 120,000 per μL and the median
71 total white blood cell count was 13,000 per μL . To rule out substantial confounding by geography
72 and age, we demonstrate the discriminatory value of platelet counts alone (Figure 1B). Low platelet
73 counts were highly predictive of blood stage parasitaemia and elevated *PfHRP2* in a cohort of 566
74 severely ill African children enrolled in the FEAST trial [21] ($p=10^{-16}$ for a spline term on the
75 \log_{10} platelet count in a generalised additive logistic regression model predicting *PfHRP2* > 1,000
76 ng/mL, Figure S1). African children enrolled in the FEAST trial who had severe thrombocytopenia
77 (< 100,000 platelets per μL) had comparable *PfHRP2* concentrations to Asian adults diagnosed
78 with severe falciparum malaria. Total white blood cell counts are age dependent and vary across
79 genetic backgrounds, in particular related to mutations in the *ACKR1* gene that results in the
80 Duffy negative phenotype prevalent in African populations [23]. However, after adjustment for age
81 (see Methods), the marginal distributions of total white counts were comparable between Asian
82 adults and children with severe malaria and African children with high *PfHRP2* (Figure S2).

83 Estimating the proportion of children mis-diagnosed with severe malaria

84 We can consider the hospitalised Kenyan children in this series as a mixture of two latent sub-
85 populations, ‘severe malaria’ and ‘not severe malaria’ (i.e an alternative aetiology for severe illness).
86 To estimate the proportion of each we use the distribution of HbAS, the human polymorphism
87 most protective against all forms of clinical falciparum malaria. HbAS provides at least 90%

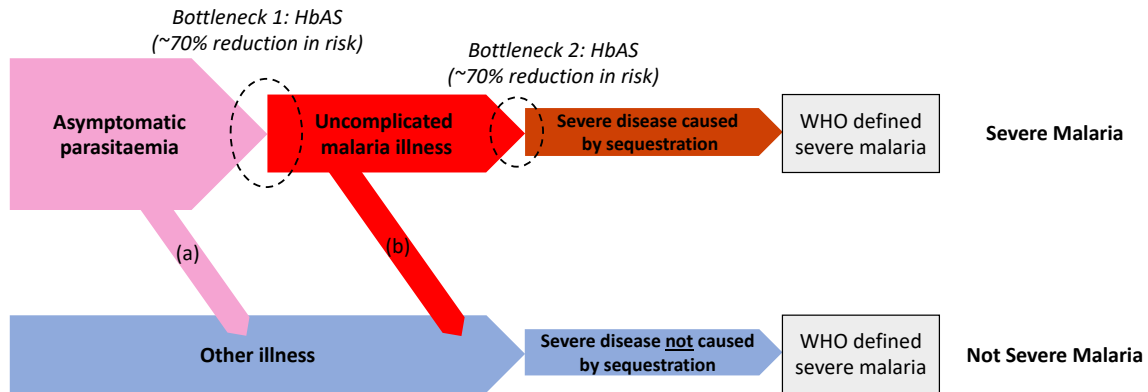


Figure 2: **Theoretical causal pathways that lead to the clinical diagnosis of severe malaria under the current WHO definition [14].** Pathways (a) & (b) represent the two ways patients can be mis-classified as severe malaria. For both pathways (a) & (b), we expect a higher prevalence of HbAS relative to the population with true severe malaria due to the protective bottlenecks. In this causal model we assume that HbAS does not protect against asymptomatic parasitaemia, although this assumption is not strictly necessary. Adapted with permission from [25].

88 protection against severe malaria [24, 6]. The causal SNP rs334 was genotyped in 2,213 of the
89 Kenyan children, of whom 57 were HbAS. The causal pathways (a) or (b) in Figure 2 (note all
90 children have been selected into the study on the basis of clinical symptoms consistent with severe
91 malaria) show how the distribution of HbAS can be used to infer the marginal probability $P(\text{Severe}$
92 $\text{malaria})$ in the Kenyan cohort as the prevalence of HbAS is expected to differ in the two latent
93 sub-populations.

94 We assumed that cases with the highest likelihood values $P(\text{Data} \mid \text{Severe malaria})$ under
95 the reference model (a bivariate t -distribution fit to the training data) had a diagnosis of severe
96 malaria that was 100% specific (top 40% of cases, a sensitivity analysis varied this threshold).
97 The cases with lower likelihood values were assumed to be drawn from a mixture of the two latent
98 populations with an unknown mixing proportion; the prevalence of HbAS in the ‘not-severe malaria’
99 subgroup was estimated from a cohort of hospitalised children enrolled in the same hospital and
100 who were malaria blood slide positive but were clinically diagnosed as not having severe malaria
101 ($n = 6,748$ of whom 364 were HbAS [26]). We assumed that this diagnosis of ‘not-severe malaria’
102 was 100% specific. Under these assumptions, we estimated that $P(\text{Severe malaria}) = 0.64$ (95%
103 credible interval (C.I.) 0.46 to 0.8), implying that approximately one third of the 2,200 cases
104 are from the ‘not-severe malaria’ sub-population (they have malaria parasitaemia in addition to
105 another severe illness - likely to be bacterial sepsis, Figure 2).

106 Estimating individual probabilities of severe malaria

107 We then estimated $P(\text{Severe malaria} \mid \text{Data})$ for each Kenyan case by fitting a mixture model to
108 the training data and to the Kenyan data jointly. The model assumed that the platelet and white
109 count data for the Kenyan children were drawn from a mixture of $P(\text{Data} \mid \text{Severe malaria})$ and
110 $P(\text{Data} \mid \text{Not severe malaria})$. The training data (Asian adults and children with severe malaria
111 and African children with $PfHRP2 > 1,000$ ng/mL) were assumed to be drawn only from $P(\text{Data}$
112 $\mid \text{Severe malaria})$. $P(\text{Data} \mid \text{Not severe malaria})$ was modelled itself as a mixture of bivariate
113 t -distributions. We used an informative prior on the mixture proportion (‘severe malaria’ versus
114 ‘not severe malaria’) in the Kenyan cases, a beta distribution approximating the posterior estimate
115 from the analysis of HbAS prevalence.

116 Figure 3A shows the bi-modal distribution of the posterior individual estimates of $P(\text{Severe}$
117 $\text{malaria} \mid \text{Data})$. The individual posterior probabilities of severe malaria were highly predictive
118 of HbAS ($p = 10^{-6}$ from a generalised additive logistic regression model fit, Figure 3C) and in-
119 hospital mortality ($p = 10^{-9}$ from a generalised additive model fit; Figure 3D). In the top quintile
120 of patients with the highest estimated $P(\text{Severe malaria} \mid \text{Data})$, the prevalence of HbAS was 0.7%
121 (3 out of 446). In contrast, for patients in the lowest quintile of estimated $P(\text{Severe malaria} \mid$
122 $\text{Data})$, the prevalence of HbAS was 4.8% (21 out of 444). These patients with a low probability

123 of severe malaria had a substantially higher case fatality ratio (6.1% mortality for patients in the
124 top quintile of $P[\text{Severe malaria} \mid \text{Data}]$ versus 18.8% mortality for the bottom quintile of $P[\text{Severe}$
125 $\text{malaria} \mid \text{Data}]$). This may be explained by the higher case-specific mortality of severe bacterial
126 sepsis (the most likely alternative cause of severe illness). The blood culture positive rate was 2.1%
127 in the top quintile of $P(\text{Severe malaria} \mid \text{Data})$, and 4.4% in the lowest quintile of $P(\text{Severe malaria}$
128 $\mid \text{Data})$ and the individual probabilities were predictive of blood culture results ($p = 0.004$ under
129 a generalised additive logistic regression model fit).

130 Accounting for case imprecision in case-control studies

131 ‘False-positive’ cases reduce statistical power and dilute effect size estimates in case-control studies.
132 We propose a novel approach for case-control studies with phenotypic imprecision based on data
133 tilting [17]. The idea is to ‘tilt’ the cases towards a pseudo-population with higher specificity for
134 severe malaria. We can do this by re-weighting the data by the probabilities $P(\text{Severe malaria} \mid$
135 $\text{Data})$, i.e. re-weighting the contribution to the log-likelihood in an association model.

136 We applied this approach as proof-of-concept to a genome-wide association study using the
137 subset of Kenyan children who had clinical and whole genome data available (after quality control
138 checks $n = 1,297$ cases) and a set of matched population controls ($n = 1,614$), across 9.6 million
139 bi-allelic variants on the autosomal chromosomes. We compared the data-tilting method to the
140 standard non-weighted approach by estimating local false discovery rates (FDR) [18]. Compared
141 to the standard non-weighted GWAS, data-tilting substantially increased the number of significant
142 associations for local FDRs in the range of 1-5% (Figure 4). For example, at an FDR of 2%,
143 the number of significant hits is more than doubled with the additional hits all around known
144 loci associated with protection from severe malaria. We note that if the data weights were not
145 predictive of the true latent phenotype, we would expect fewer significant hits for a given FDR
146 due to the reduction in effective sample size. This is demonstrated by permuting the data weights
147 (for the cases only), which results in 50-75% reduction in the number of significant hits at a FDR
148 of 5% (Figure S3).

149 Examining the three major genetic regions strongly associated with protection from severe
150 malaria in East Africa (*HBB*: HbAS; *ABO*: O blood group; *FREM3*: Dantu blood group) [7], the
151 data-tilted approach estimated larger effect sizes compared to the non-weighted model in all three
152 regions (effect size increases: 30% around *HBB*, 9% around *ABO*, and 5% around *FREM3*). This
153 resulted in larger $-\log_{10}$ p-values for *HBB* and *ABO*, but slightly smaller for *FREM3* (Figure 5).

154 Reappraisal of directly typed polymorphisms

155 We re-analysed 120 polymorphisms on 70 candidate malaria-protective genes which were typed
156 directly in the 2,220 Kenyan children along with 3,940 population controls. In this case-control
157 cohort, 14 polymorphisms had previously been identified as associated with protection or increased
158 risk in severe malaria [27]. A re-analysis of these 14 variants using the same models of association
159 as previously published and down-weighting the likely mis-classified cases replicated the major-
160 ity of associations, with increased effect sizes and increased $-\log_{10}$ p-values (Figure S4). For the
161 three major genes (*HBB*, *ABO*, *FREM3*), effect sizes were increased by 10-30% and associations
162 all had higher significance levels on the $-\log_{10}$ scale (0.25-1.7). The allele frequencies of all three
163 polymorphisms were directly associated with the probability weights, showing increased protection
164 in individuals more likely to have severe malaria (Figure S5). Two polymorphisms on the genes
165 *ARL14* and *LOC727982*, reported previously as associated with protection in severe malaria (nei-
166 ther of which are related to red cells), showed decreased effect sizes and $-\log_{10}$ p-values and are
167 thus potentially spurious hits.

168 We explored whether there was evidence of differential effects in the Kenyan cases using $P[\text{Severe}$
169 $\text{malaria} \mid \text{Data}]$ to assign probabilistically each case to the ‘severe malaria’ versus ‘not severe
170 malaria’ sub-populations. We fitted a categorical logistic regression model predicting the latent sub-
171 population label versus control, where the latent case label was estimated from the weights shown
172 in Figure 3A. This resulted in approximately 1,279 cases in the ‘severe malaria’ sub-population and
173 941 cases in the ‘not severe malaria’ sub-population. Differential effects were tested by comparing
174 the estimated log-odds for the two sub-populations. After accounting for multiple testing, two
175 polymorphisms showed significant differential effects: rs334 (derived allele encodes haemoglobin
176 S, $p = 10^{-6}$) and rs1050828 (derived allele encodes *G6PD*+202T, $p = 10^{-3}$ in the model fit

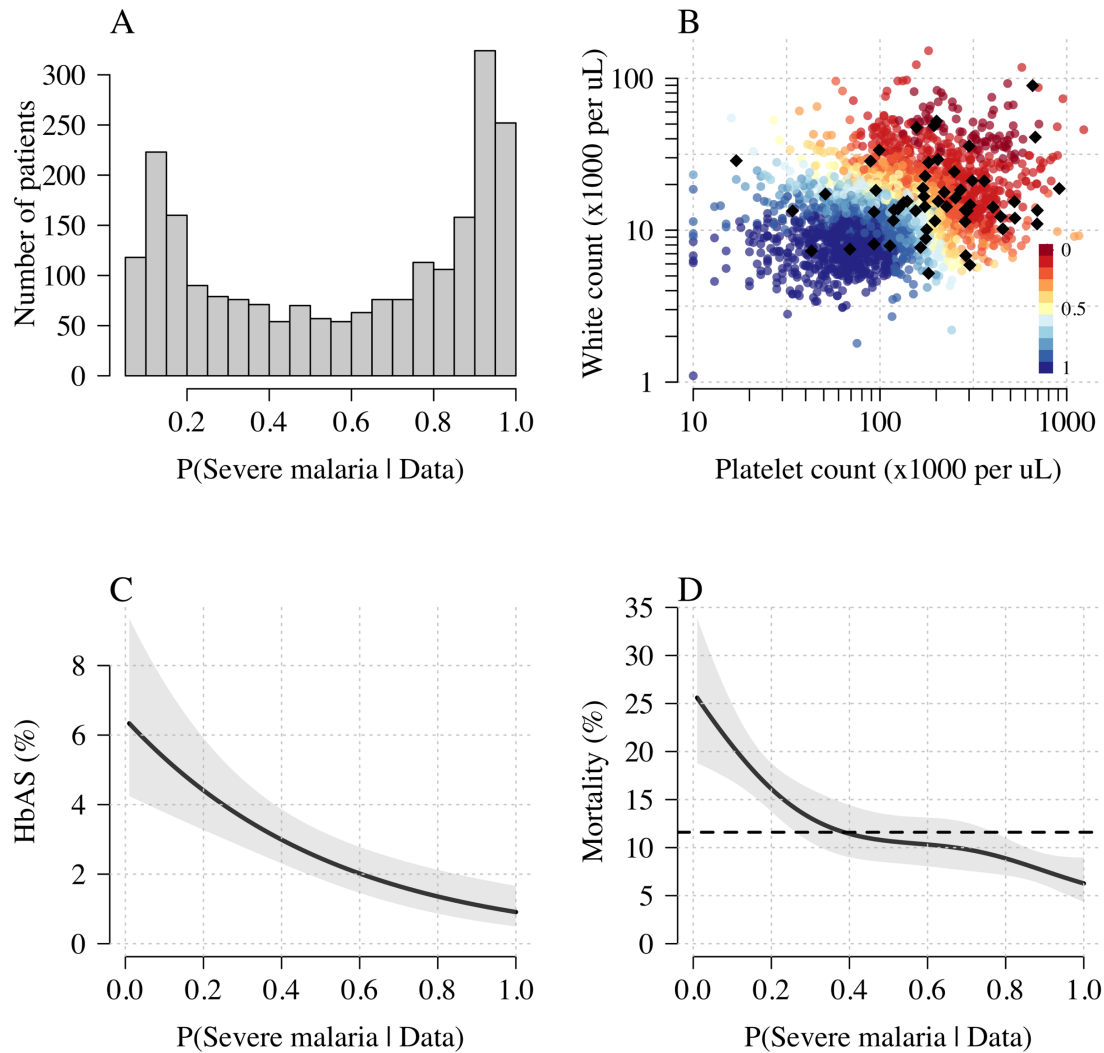


Figure 3: **Model estimates of $P(\text{Severe malaria} \mid \text{Data})$ in 2,220 Kenyan children clinically diagnosed with severe malaria.** Panel A: distribution of posterior probabilities of severe malaria being the correct diagnosis. Panel B shows these probabilities plotted as a function of the platelet and white counts on which they are based. The black diamonds show the HbAS individuals. Panels B & C show the relationship between the estimated probabilities of severe malaria and HbAS and in-hospital mortality. The black lines (shaded areas) show the mean estimated values (95% confidence intervals) from a generalised additive logistic regression model with a smooth spline term for the likelihood (R package *mgcv*).

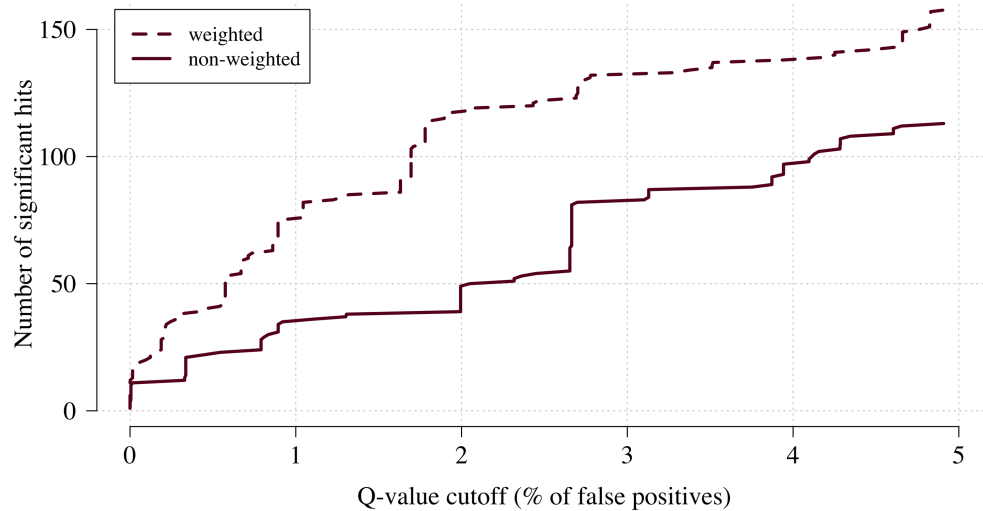


Figure 4: **The number of significant hits as a function of the false discovery rate for the genome-wide association study across 9.6 million bi-allelic variants.** This analysis is based on a subset of the Kenyan children with whole genome data available and passing quality checks $n = 1,297$, and $n = 1,614$ controls. Dashed line: weighted-model; thick line: non-weighted model.

177 to females only), see Figure 6. As expected, rs334 was associated with protection in both sub-
178 populations [28, 26] but the effect was almost 8 times larger on the log-odds scale in the ‘severe
179 malaria’ sub-population relative to the ‘not severe malaria’ sub-population (odds-ratio of 0.029
180 [95% C.I. 0.0088-0.094] in the ‘severe malaria’ population versus 0.63 [95% C.I. 0.48-0.83] in the
181 ‘not severe malaria’ population). For rs1050828 (*G6PD*+202T allele), approximately the same
182 absolute log-odds were estimated for both sub-populations but they had opposite sign. Under an
183 additive model in females, the rs1050828 T allele was associated with protection in the ‘severe
184 malaria’ sub-population (odds-ratio of 0.71 [95% C.I. 0.57-0.88]) but with increased risk in the
185 ‘not severe malaria’ sub-population (odds-ratio of 1.30 [95% C.I. 1.00-1.70]). The additive model
186 including both males and females was consistent with these opposing effects but significant only
187 at a nominal threshold ($p = 0.02$). Opposing effects across the two sub-populations is consistent
188 with the hypothesis that G6PD deficiency leads to a greater risk of being erroneously classified
189 as severe malaria due to the severe anaemia criterion [29] (shown in more detail in Figure S5).
190 Investigation of haemoglobin concentrations as a function of $P(\text{Severe malaria} \mid \text{Data})$ indicates
191 that the mis-classified group is very heterogeneous, but with a larger proportion of severe anaemia
192 (<5 g/dL) relative to the correctly classified sub-population (Figure S6).

193 Discussion

194 The clinical diagnosis of severe falciparum malaria in African children is imprecise [10, 11, 9].
195 Even with quantitation of parasite densities, specificity is still imperfect [11]. In children with
196 cerebral malaria (unrousable coma with malaria parasitaemia), the most specific of the severe
197 malaria clinical syndromes, post-mortem examination revealed another diagnosis in about 25% of
198 cases studied in Blantyre, Malawi [10]. Diagnostic specificity can be improved by visualisation of
199 the obstructed microcirculation in-vivo (e.g. through indirect ophthalmoscopy) or from parasite
200 biomass indicators (quantitation and staging of malaria parasites on thin blood films, counting of
201 neutrophil ingested malaria pigment, measurement of plasma concentrations of *Pf*HRP2 or parasite
202 DNA), but these are still largely research procedures and have not been widely adopted or measured
203 at scale for genetic association studies. Our results suggest that imprecision in clinical phenotyping
204 is more substantial than thought previously. In this cohort of 2,220 Kenyan children diagnosed
205 with severe malaria from an area of moderate transmission, a probabilistic assessment suggests that

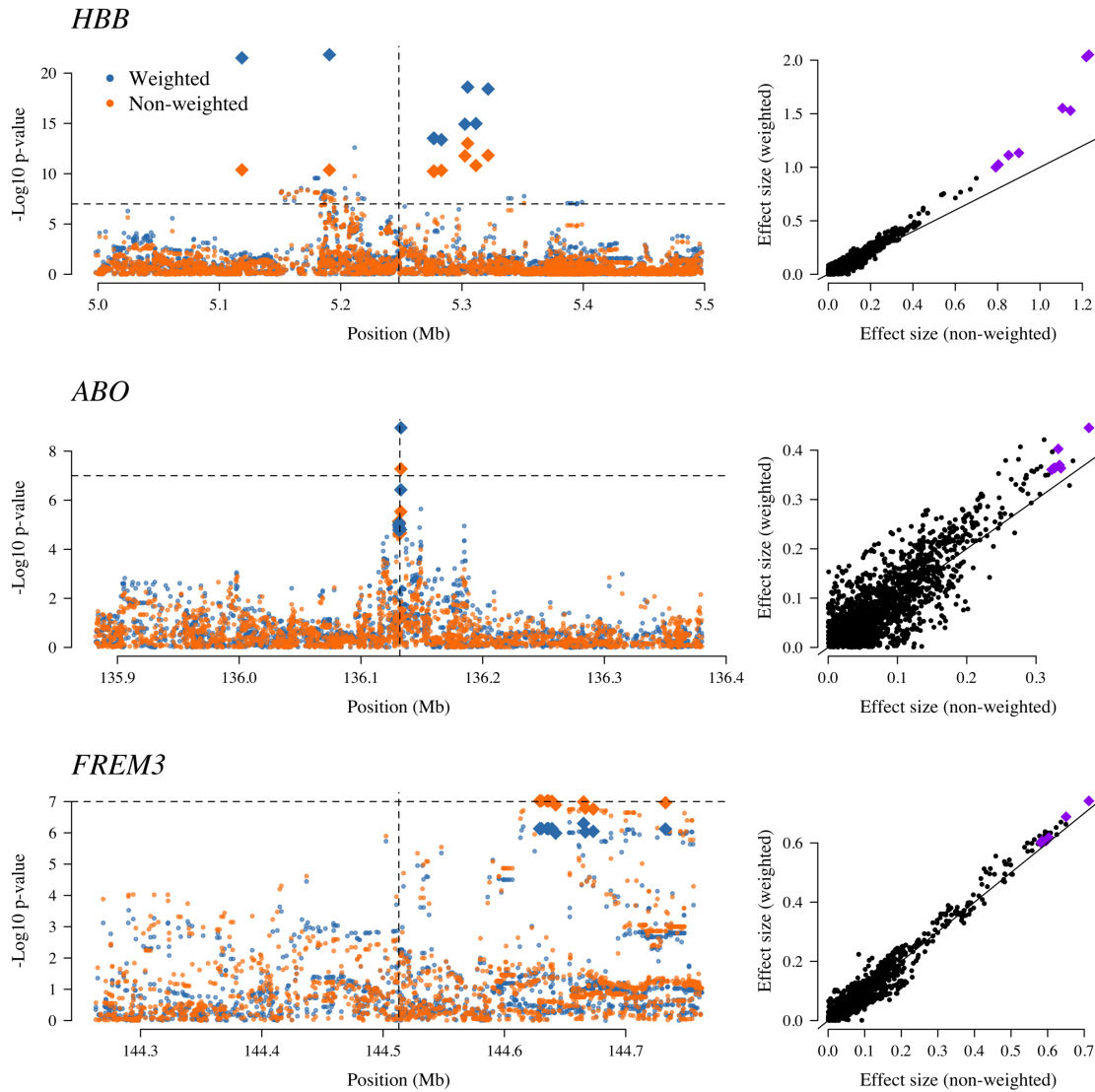


Figure 5: **The three regions in the human genome with the greatest evidence for protection against severe malaria in East Africa (*HBB*, *ABO* and *FREM3*) [7].** The Manhattan plots (left panels) compare p-values from the weighted model (blue) and the non-weighted model (orange). Each Manhattan plot is centred around the known causal position shown by the vertical dashed line (0.5 Mb region). The horizontal dashed line shows $p = 10^{-7}$ (threshold often used for defining genome-wide significance). The 10 positions with the greatest $-\log_{10}$ p-values under the non-weighted model are shown as large diamonds. The scatter plots on the right compare absolute effect size estimates under both models with the same top 10 hits shown by the larger purple diamonds. Increases of 30%, 9% and 5% are seen for the ten top hits for *HBB*, *ABO*, and *FREM3*, respectively.

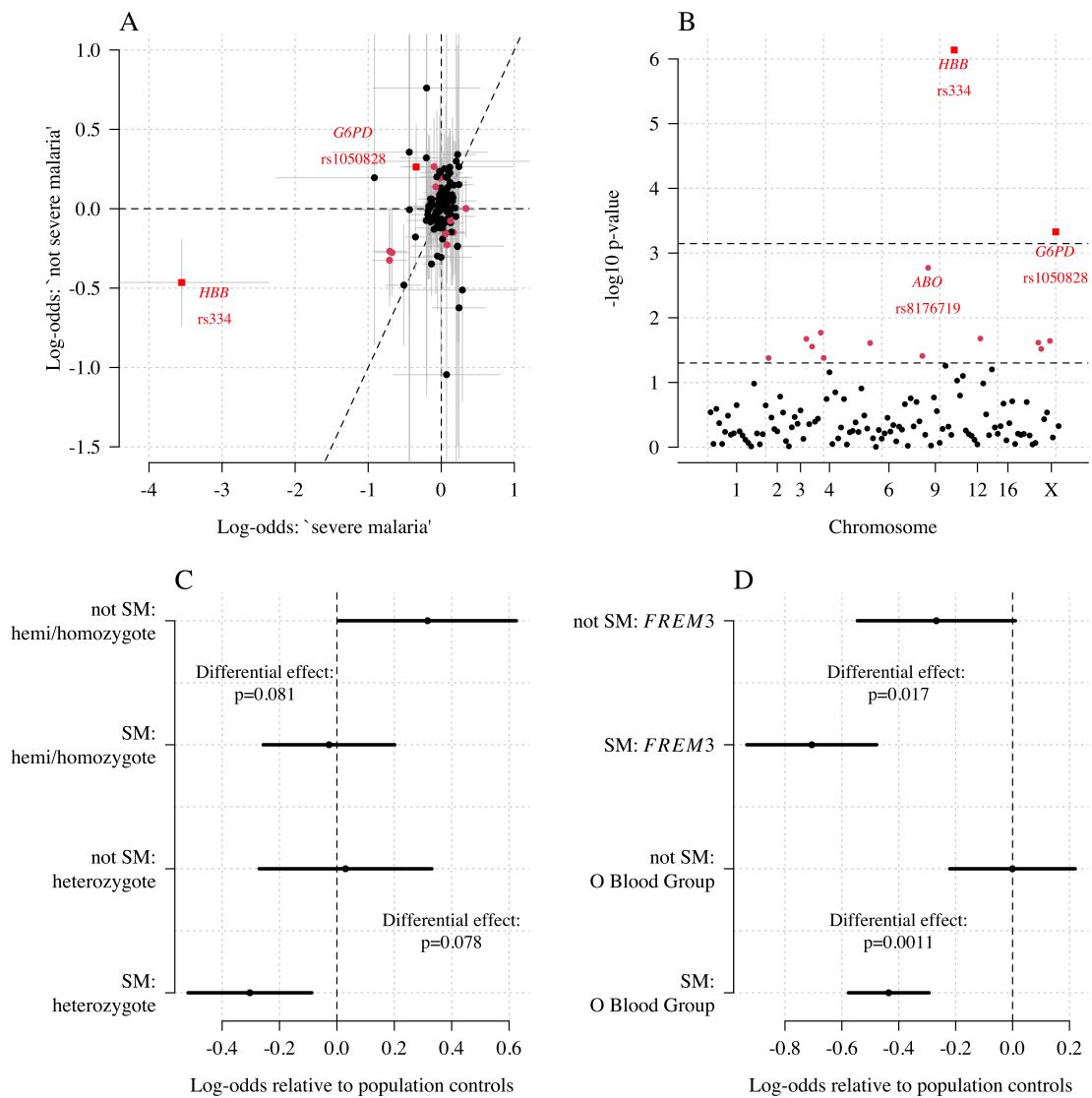


Figure 6: Exploring differential effects in 120 directly typed polymorphisms across 70 candidate malaria-protecting genes. Panel A: case-control effect sizes estimated for the ‘severe malaria’ sub-population versus the ‘not severe malaria’ sub-population ($n = 3,940$ controls and $n = 2,220$ cases, with approximately 1,279 in the ‘severe malaria’ sub-population and 941 in the ‘not severe malaria’ sub-population). The vertical and horizontal grey lines show the 95% credible intervals. Panel B shows the \log_{10} p-values testing the hypothesis that the effects are the same for the two sub-populations relative to controls. The top dashed line shows the Bonferroni corrected $\alpha = 0.05$ significance threshold (assuming 70 independent tests). The bottom dashed line shows the nominal $\alpha = 0.05$ significance threshold. In both panels, red circles denote $p < 0.05$ (nominal significance level), and red squares denote $p < 0.05/70$. Panel C: Analysis of the rs1050828 SNP (encoding G6PD+202T) under a non-additive model (hemi/homozygotes and heterozygotes are distinct categories). This shows that heterozygotes are clearly under-represented in the ‘severe malaria’ sub-population and hemi/homozygotes are clearly over-represented in the ‘not severe malaria’ sub-population. Panel D: evidence of differential effects for the O Blood Group (rs8176719, recessive model) and *FREM3* (additive model).

206 over one third may not have had severe malaria (although malaria may have contributed to their
207 illness [25]). This supports our previous conclusion that differences in treatment effects between
208 Asian adults and African children (i.e the benefits of artesunate over quinine in severe malaria
209 estimated from randomised trials [30, 31]) are predominantly driven by differences in diagnostic
210 specificity [22, 9]. Using HbAS as a natural experiment to validate the biomarker model, we show
211 that the joint distribution of platelet and white blood cell counts is a diagnostic predictor of severe
212 malaria. Complete blood counts are inexpensive and increasingly available in low-resource setting
213 hospitals. An upper threshold of 200,000 platelets per μL would have substantially decreased
214 mis-classification in this large cohort of Kenyan children diagnosed with severe malaria.

215 Our re-analysis using rich clinical data provides additional evidence for the three major genetic
216 polymorphisms present in East Africa which are the most highly protective against severe malaria.
217 After probabilistic down-weighting of the likely mis-classified cases substantial increases in effect
218 sizes were found. Dilution of effect sizes resulting from mis-classification could explain the large
219 heterogeneity in effects noted in the largest severe malaria GWAS to date [7]. For haemoglobin
220 S (rs334) there was a 4-fold variation in estimated odds-ratios across participating sites. Some of
221 this heterogeneity can be attributed to variations in linkage disequilibrium affecting imputation
222 accuracy [5], but our analysis shows an additional substantial source of heterogeneity which results
223 from diagnostic imprecision. This can be adjusted for if detailed clinical data are available. For
224 example, in the case of rs334 (directly typed), the data-tilting approach results in a 25% increase
225 in effect size on the log-odds scale, corresponding to 35% decrease in estimated odds-ratios (0.1
226 versus 0.16).

227 As for the interpretation of genetic effects, one of the most interesting results concerns the
228 *G6PD* gene. G6PD deficiency is the most common enzymopathy of humans, and its role in falciparum
229 malaria has been controversial [32, 29]. A very large multi-country genetic association study
230 with over 11,000 severe malaria cases and 17,000 population controls found no overall protective
231 effect of the *G6PD*+202T allele (the most common mutation in sub-Saharan Africa causing G6PD
232 deficiency), under an additive model [6]. The same pattern is observed in this Kenyan cohort
233 (which is a subset of the larger study). In the Kenyan cohort overall, a previous analysis found no
234 clear evidence of protection for male homozygotes but substantial evidence of protection for female
235 heterozygotes [33]. This suggests a heterozygote advantage leading to a balancing polymorphism.
236 However, when the Kenyan cases are modelled as two distinct sub-populations, there is evidence of
237 differential effects between the ‘severe malaria’ and ‘not severe malaria’ sub-populations. Hemi and
238 homozygous G6PD deficiency was associated with an increased risk of mis-classification (reflecting
239 an increased risk of severe anaemia), but it is unclear whether or not hemi/homozygous G6PD
240 deficiency was protective in the ‘true severe malaria’ sub-population (Figure 6C). On the other
241 hand, heterozygote deficiency was very clearly protective in the true severe malaria subgroup, con-
242 sistent with previous findings, and did not appear to lead to an increased risk of mis-classification
243 (consistent with a lower risk of extensive haemolysis and thus false classification in heterozygotes
244 who have both normal and G6PD deficient erythrocytes in their circulation). When examining
245 the ‘severe malaria’ sub-population only, the sample size in this study is too small to discriminate
246 between the heterozygote and additive models of association. In our view, the relationship between
247 G6PD deficiency and severe falciparum malaria remains unanswered. This approach should now
248 be applied to other case-control cohorts for a definitive understanding of the role of this major
249 human polymorphism.

250 The limitations of our diagnostic model can be summarised as follows. First, the validity
251 and interpretation of the individual probabilities that severe malaria is the correct diagnosis is
252 heavily dependent on the reference model and thus the training data. Our training data were
253 primarily from Asian adults in whom diagnostic specificity for severe malaria is thought to be very
254 high. Diagnostic checks suggested that the marginal distributions of platelet counts were similar
255 between adults and children, and we made age corrections to the white blood cell count, but small
256 deviations could reduce the discriminatory value (e.g. lower white counts associated with the
257 Duffy negative phenotype [23]). Second, it is possible that rare genetic conditions exist in which
258 the probabilities of severe malaria under this model might be biased. One example is sickle cell
259 disease (HbSS, <0.5% in the Kenyan cases), which results in chronic inflammation with high white
260 counts and low platelet counts relative to the normal population [34]. The 11 children with HbSS
261 in this cohort were all assigned low probabilities of severe malaria, but this should be interpreted
262 with caution. Whether HbSS is protective against severe malaria or increases the risk of severe
263 malaria remains unclear [35]. For these patients, other biomarkers such as plasma *PfHRP2* may

264 be more appropriate. Third, it is theoretically possible that the joint distribution of the clinical
265 variables used to fit the reference model could be dependent on the underlying distribution of
266 severe malaria sub-phenotypes. For example, if the training data were biased towards cerebral
267 malaria, and the joint distribution of platelet and white cell counts in cerebral malaria differed
268 from those in the other severe malaria syndromes, then the predicted outliers could represent other
269 forms of severe malaria instead of ‘not-severe’ malaria. This would not impact the estimate of 1 in
270 3 mis-classification unless the protective effect of HbAS varied substantially amongst the different
271 sub-phenotypes of severe malaria. This variation has not been noted in previous analyses [7].

272 In summary, under a probabilistic model based on routine blood count data, we have shown
273 that it is possible to estimate mis-classification rates in diagnosed severe childhood malaria in
274 a higher transmission endemic area and compute probabilistic weights that can downweight the
275 contribution of likely mis-classified cases. The well-established protective effect of HbAS provided
276 an independent validation of the model. These data suggest that normal range platelet counts
277 ($> 200,000$ per μL) could be used as a simple exclusion criterion in severe malaria cohort studies.
278 Based on this analysis we recommend that future studies in severe malaria collect and record
279 complete blood count data. Further studies of platelet and white blood cell counts from a diverse
280 cohort of children with severe malaria, confirmed using high specificity diagnostic techniques such
281 as indirect ophthalmoscopy, plasma *PfHRP2*, or plasma *P. falciparum* DNA should be conducted
282 to validate this approach.

283 **Methods**

284 **Data**

285 **Kenyan case-control cohort**

286 The Kenyan case-control cohort has been described in detail previously [27]. Severe malaria cases
287 consisted of all children aged <14 years who were admitted with clinical features of severe falciparum
288 malaria to the high dependency ward of Kilifi County Hospital between June 11th 1999
289 and June 12th 2008. Severe malaria was defined as a positive blood-film for *P. falciparum* along
290 with: prostration (Blantyre Coma Score of 3 or 4); cerebral malaria (Blantyre Coma Score of
291 <3); respiratory distress (abnormally deep breathing); severe anaemia (haemoglobin < 5 g/dL).
292 Controls were infants aged 3-12 months who were born within the same area as the cases and who
293 were recruited to a cohort study investigating genetic susceptibility to a wide range of childhood
294 diseases. Cases and controls were genotyped for the rs334 SNP and for α^+ -thalassaemia along with
295 120 other SNPs using DNA extracted from fresh or frozen samples of whole blood as described in
296 detail previously [27, 36].

297 **The Fluid Expansion as Supportive Therapy (FEAST) trial**

298 FEAST was a multicentre randomised controlled trial comparing fluid boluses for severely ill chil-
299 dren ($n = 3,161$) that was not specific to severe malaria [21]. Platelet counts, white blood cell
300 counts, parasite densities and *PfHRP2* were jointly measured for 566 children (for children enrolled
301 in the sites in Mulago, Lacor and Mbale, Uganda). In order to select only those with a very high
302 probability of having severe malaria as the primary cause of illness, we selected the 121 children
303 who had measured *PfHRP2* $> 1,000$ ng/mL and parasitaemia $> 1,000$ per μL .

304 **AQ Vietnam and AAV randomised controlled trials**

305 The AQ and the AAV studies were two randomised clinical trials in Vietnamese adults diagnosed
306 clinically with severe falciparum malaria recruited to a specialist ward of the Hospital for Tropical
307 Diseases, Ho Chi Minh City, Vietnam, between 1991 and 2003 [19, 20]. AQ Vietnam was a
308 double blind comparison of intramuscular artemether versus intramuscular quinine ($n = 560$);
309 AAV compared intramuscular artesunate and intramuscular artemether ($n = 370$).

310 **Observational studies in Thai and Bangladeshi adults and children**

311 We included data from multiple observational studies in severe falciparum malaria conducted by
312 the Mahidol Oxford Tropical Medicine Research Unit in Thailand and Bangladesh between 1980

313 and 2019. These pooled data have been described previously [37]. Platelet counts and white blood
314 cell counts were available in 657 patients. We excluded one 30 year old adult from Bangladesh
315 whose recorded platelet count was 1,000 per μL , and three other adults with platelet counts greater
316 than 450,000 per μL as outliers reflecting likely data entry errors. Plasma *Pf*HRP2 concentrations
317 were available in 172 patients from Bangladesh. 55 patients from this series were younger than 15
318 years of age.

319 Multiple imputation

320 In the Kenyan severe malaria cohort ($n = 2,220$), data on platelet counts were missing in 18%,
321 white blood counts were missing in 0.2%, and parasite density was missing in 1.6%. In-hospital
322 outcome (died/survived) was missing for 13 patients. rs334 genotype was missing for 7; α^+ -
323 thalassaemia genotype was missing for 101 patients. In the Vietnamese adults, platelet counts
324 were missing in 4%, white counts in 2% and parasitaemia in 0%.

325 We did multiple imputation using random forests for all available clinical variables using the
326 R package *missForest* (targeted genotyping data was not included for imputation). Supplemen-
327 tary Figures S7 and S8 shows the missing data pattern in the studies in Vietnamese adults and
328 in the Kenyan severe malaria cases, respectively. Ten datasets were imputed for each dataset
329 independently and were used for the subsequent analyses. Analyses using directly typed genetic
330 polymorphisms or the within-hospital outcome as the dependent variables used only the data where
331 these outcomes were recorded, assuming that they were missing at random.

332 Reference model of severe malaria

333 Biological rationale

334 Thrombocytopenia accompanied by a normal white blood count and a normal neutrophil count
335 are typical features of severe malaria [38, 39], but they may also occur in some systemic viral
336 infections and in severe sepsis. Neutrophil leukocytosis may sometimes occur in very severe malaria,
337 but is more characteristic of pyogenic bacterial infections. These indices, whilst individually not
338 very specific, could each have useful discriminatory value. We reasoned therefore that their joint
339 distribution could help discriminate between children with severe malaria versus those severely ill
340 with coincidental parasitaemia. The Kenyan severe malaria cohort did not have differential white
341 count data, so we used platelet counts and total white blood cell counts as the two diagnostic
342 biomarkers in the reference model of severe malaria.

343 Choice of training data and confounders

344 The best data for fitting the biomarker model are either from children or adults from low transmis-
345 sion areas (where parasitaemia has a high positive predictive value); or in children or adults with
346 high plasma *Pf*HRP2 measurements indicating a large latent parasite biomass [22]. In the first
347 years of life, white blood cell counts are often much higher than in adults because of lymphocytosis.
348 We used data from 858 children from the FEAST trial, in whom white counts were measured, to
349 estimate the relationship between age and mean white count in severe illness (median age was 24
350 months). The estimated relationship is shown in Figure S9 (using a generalised additive linear
351 model with the white count on the \log_{10} scale), with mean white counts reaching a plateau around
352 5 years of age. We used this to correct all white count data in children less than 5 years of age,
353 both in the training data and the Kenyan cohort.

354 There is also a systematic difference associated with the Duffy negative phenotype which is
355 near fixation in Africa but absent in Asia. Duffy negative individuals have lower neutrophil counts
356 (termed benign ethnic neutropenia) [23]. The use of Asian adults to estimate the reference distri-
357 bution of white counts in severe malaria could thus falsely include individuals with elevated white
358 counts (relative to the normal ranges). However, a diagnostic quantile-quantile plot (Figure S2, on
359 the log-scale) comparing the white count distribution in Vietnamese adults and in children in the
360 FEAST trial who had *Pf*HRP2 $> 1,000$ ng/mL did not suggest any major differences. In fact the
361 African children had slightly higher white counts on average even after the correction for age, this
362 may represent imperfect specificity when using a plasma *Pf*HRP2 cutoff of 1,000 mg/mL.

363 For platelet counts (which have the greatest diagnostic value for severe malaria in our series)
364 age is not a confounder and published data support the hypothesis that thrombocytopenia is highly

365 specific for severe malaria in children as well as adults (with a diagnostic and a prognostic value).
366 The French national guidelines specifically mention thrombocytopenia ($<150,000$ per μL) for the
367 diagnosis of children who have travelled to a malaria endemic area. In a French paediatric series
368 in travellers, almost half had severe thrombocytopenia ($<50,000$ per μL) [40, 41]. In Dakar,
369 Senegal (one of the lowest transmission areas in Africa) thrombocytopenia was an independent
370 predictor of death and the median platelet count was 100,000 [42, 43]. Comparison of the distributions
371 of platelet counts (on the log scale) between Asian children and Asian adults suggested
372 no major differences (Figure S10), although we had few data for Asian children. In the seminal
373 Blantyre autopsy study [10], platelet counts were substantially different between fatal cases confirmed
374 post-mortem to be severe malaria (62,000 per μL , and 56,000 per μL for the children with
375 sequestration only, and for sequestration + microvascular pathology, respectively) and fatal cases
376 with a mis-diagnosis of severe malaria (no sequestration: 176,000 per μL ; the inter-group difference
377 was significant, $p = 0.008$). A larger cohort from the same centre in Malawi reported substantially
378 higher platelet counts in retinopathy negative cerebral malaria (mean count was 161,000 per
379 μL , $n = 288$) compared to retinopathy positive cerebral malaria (mean count was 81,000 per μL ,
380 $n = 438$) [25].

381 We visually checked approximate normality for each marginal distribution using quantile-
382 quantile plots (Figure S11). On the \log_{10} scale, platelet counts and white counts show a good
383 fit to the normal approximation but with some outliers so a t -distribution was used (robust to out-
384 liers). For all modelling of the joint distribution of platelet counts and white blood cell counts, we
385 chose bivariate t -distributions with 7 degrees of freedom as the default model. The final reference
386 model used was a bi-variate t -distribution fit to the joint distribution of platelet counts and white
387 counts both on the logarithmic scale. On the \log_{10} scale the mean values (standard deviations)
388 were approximately 1.76 (0.11) and 0.92 (0.055) for platelets and white counts, respectively. The
389 covariance was approximately 0.0035. These values varied very slightly across the ten imputed
390 datasets. Log-likelihood values for each severe malaria case in the Kenyan cohort were calculated
391 for each imputed dataset independently. The median log-likelihoods per case were then used in
392 downstream analyses.

393 Limitations of the model

394 The diagnostic model of severe malaria using platelet counts and white blood cell counts cannot be
395 applied to all patients. We summarise here the known and possible limitations. When using this
396 model to estimate the association between a genetic polymorphism and the risk of severe malaria,
397 if the genetic polymorphism of interest affects the complete blood count independently, there will
398 be selection bias (see the directed acyclic graph in Figure S12). One example is HbSS. Children
399 with HbSS have chronic inflammation with white blood cells counts about 2-3 times higher than
400 normal and slightly lower platelet counts [34]. All 11 children in the Kenyan cohort with HbSS
401 were assigned low probabilities of having severe malaria (Figure S13), but these probabilities reflect
402 a deficiency of the model. Including or excluding these children from the analysis had no impact
403 on the results as they represent less than 0.5% of the cases.

404 The second possible limitation concerns the validation using HbAS. Previous studies have sug-
405 gested negative epistasis between the malaria-protective effects of HbAS and α^+ -thalassaemia
406 [44, 45]. The 3.7 kb deletion across the *HBA1-HBA2* genes (known as α^+ -thalassaemia) has an
407 allele frequency of $\sim 40\%$ in this population, therefore 16% of HbAS individuals are homozygous
408 for α^+ -thalassaemia [46]. Negative epistasis implies that those with both polymorphisms would
409 have less or no protective effect against severe malaria. Of the 2,113 Kenyan cases with both HbS
410 and α^+ -thalassaemia genotyped, 13 were HbAS and homozygous α^+ -thalassaemia. Figure S14
411 shows that the majority of those with both polymorphisms had clinical indices pointing away from
412 severe malaria suggesting that the observed number of patients with both HbAS and homozygous
413 α^+ -thalassaemia is inflated by 2 to 3 fold.

414 The final possible problem concerns the use of white blood cell counts in relation to invasive
415 bacterial infections. Bacteraemia could either be the cause of severe illness (with coincidental
416 parasitaemia), or it could be concomitant (which may result from extensive parasitised erythrocyte
417 sequestration in the gut), i.e. a result of severe malaria. The former should be identified as ‘not-
418 severe malaria’ (as bacteraemia is the main cause of illness), but the latter should be identified as
419 ‘severe malaria’ and might be mis-classified as ‘not-severe malaria’ under our model. However, in
420 a series of 845 Vietnamese adults (high diagnostic specificity), only one of eight patients who had
421 concomitant invasive bacterial infections and a white count measured had leukocytosis (median

422 white count was 8,100; range 3,500 to 14,850) [47].

423 Estimating the diagnostic specificity in the Kenyan cohort

424 We assume that the Kenyan cases are a latent mixture of two sub-populations: P_0 is the population
425 ‘severe malaria’ and P_1 is the population ‘not-severe malaria’ (mis-classified). For diagnostic
426 biomarkers X , this implies that $X \sim G = \pi f_0 + (1-\pi)f_1$, where f_0, f_1 are the sampling distributions
427 (likelihoods) of each sub-population, respectively.

428 We can infer the value of π (proportion correctly classified as severe malaria) without making
429 parametric assumptions about f_1 by using the distribution of HbAS (see Figure 2). This done
430 as follows. We first estimate \hat{f}_0 by fitting a bivariate t -distribution to the training data - this
431 approximates the sampling distribution for P_0 . We then make three assumptions:

- 432 1. Out of the 2,213 Kenyan cases with rs334 genotyped, we assume that cases in the top 40th
433 percentile of the likelihood distribution under f_0 are drawn from P_0 : $N_0 = 887$, of which
434 $N_0^{sickle} = 9$ are HbAS.
- 435 2. For the other cases the proportion drawn from P_0 is unknown and denoted π' : $N_G = 1,326$,
436 of which $N_G^{sickle} = 48$ are HbAS.
- 437 3. Finally, additional information is incorporated by using data from a cohort of individuals
438 with severe disease from the same hospital who had positive malaria blood slides but whose
439 diagnosis was not severe malaria ($N_1 = 6,748$, of which $N_1^{sickle} = 364$ were HbAS) [26].

440 Under these assumptions, we can fit a Bayesian binomial mixture model to these data with
441 three parameters: $\{\pi', p_0, p_1\}$. The likelihood is given by: $N_0^{sickle} \sim \text{Binomial}(p_0, N_0)$; $N_G^{sickle} \sim$
442 $\text{Binomial}(\pi'p_0 + (1-\pi')p_1, N_G)$; $N_1^{sickle} \sim \text{Binomial}(p_1, N_1)$ The priors were: $p_1 \sim \text{Beta}(5, 95)$
443 (i.e. 5% prior probability with 100 pseudo observations); $p_0 \sim \text{Beta}(1, 99)$ (1% prior probability
444 with 100 pseudo observations). A sensitivity analysis with flat beta priors ($\text{Beta}[1,1]$) did not
445 qualitatively change the result (by one percentage point for the final estimate of π). To check
446 the validity of the use of the external population from [26], we did a sensitivity analysis using the
447 lowest quintile of the likelihood ratio distribution as a population drawn entirely from P_1 (instead
448 of the external data from [26]).

449 Estimating P(Severe malaria | Data) in the Kenyan cohort

Denote the platelet and white count data from the FEAST trial as $\{X_i^{\text{FEAST}}\}_{i=1}^{121}$; the data from the
Vietnamese adults and children as $\{X_i^{\text{Asia}}\}_{i=1}^{1583}$; the data from the Kenyan children as $\{X_i^{\text{Kenya}}\}_{i=1}^{2220}$.
We fit the following joint model to the training biomarker data and the Kenyan biomarker data.

$$\begin{aligned} X_i^{\text{FEAST}} &\sim \text{Student}(\mu_{SM}^1, \Sigma_{SM}^1, 7) \\ X_i^{\text{Asia}} &\sim \text{Student}(\mu_{SM}^2, \Sigma_{SM}^2, 7) \\ X_i^{\text{Kenya}} &\sim \pi f_0 + (1-\pi)f_1 \\ f_0 &= p \text{Student}(\mu_{SM}^1, \Sigma_{SM}^1, 7) + (1-p) \text{Student}(\mu_{SM}^2, \Sigma_{SM}^2, 7) \\ f_1 &= \sum_{j=1}^K \alpha_j \text{Student}(\mu_{notSM}^j, \Sigma_{notSM}^j, 7) \end{aligned}$$

with the following prior distributions and hyperparameters, where $\alpha = \{\alpha_1, \dots, \alpha_K\}$ such that
 $\sum_{j=1}^K \alpha_j = 1$:

$$\begin{aligned} \pi &\sim \text{Beta}(40.3, 24.7) \\ p &\sim \text{Beta}(2, 2) \\ \mu_{SM}^{1,2} &\sim \text{Normal}(\{1.8, 0.95\}, 0.1^2) \\ \mu_{notSM}^{1..K} &\sim \text{Normal}(\{2.5, 1.5\}, 0.25^2) \\ \alpha &\sim \text{Dirichlet}(1/K, \dots, 1/K) \end{aligned}$$

450 The covariance matrices $\Sigma_{SM}^{1,2}$ and $\Sigma_{SM}^{1..6}$ were parameterised as their Cholesky LKJ decomposi-
451 tion, where the L correlation matrices had a uniform prior (i.e. hyperparameter $\nu=1$). The model
452 was implemented in *rstan*.

453 This models the biomarker data in ‘not severe malaria’ as a mixture of K t -distributions. We
454 chose $K = 6$ as the default choice (sensitivity analysis increasing this has no impact). The Dirichlet
455 prior with hyperparameter $1/K$ forces sparsity in this mixture model (most of the prior weight is on
456 the vertices of the K -dimensional simplex), see for example [48]. This is a very general and flexible
457 way of modelling the ‘not severe malaria’ distribution: we are not trying to make inferences about
458 this distribution, we just want the mixture model to be flexible enough to describe it. The model
459 also allows for differences in the joint distribution of platelet counts and white counts between the
460 training datasets (FEAST trial and the Asian studies). The Kenyan cases drawn from the ‘severe
461 malaria’ sub-population are then modelled as a mix of these two training models.

462 Reweighted likelihood for case-control analyses

463 For each $\{X_i^{\text{Kenya}}\}_{i=1}^{2220}$ we estimate the posterior probability of being drawn from the sampling
464 distribution f_0 . The mean posterior probability then defines a precision weight w_i which can be used
465 in a standard generalised linear model (glm) with the same interpretation as inverse probability
466 weights. The weighted glm is equivalent to computing the maximum likelihood estimate where the
467 log-likelihood is weighted by w_i . In our case-control analyses all the controls are given weight 1.
468 Nie *et al* [17] give a proof of correctness for this re-weighted log-likelihood (equivalent to ‘tilting’
469 the dataset towards the desired distribution $\hat{f}_0(X)$).

470 Genome-wide association study

471 Anonymised whole genome data from the Illumina Omni 2.5M platform for 1,944 severe malaria
472 cases and 1,738 population controls were downloaded from the European Genome-Phenome Archive
473 (dataset accession ID: EGAD00010001742, release date March 2019 [7]). This contained sequencing
474 data on 2,383,648 variants. We used the quality control meta-data provided with the 2019 data
475 release to select SNPs and individuals with high quality data. We first excluded 386 individuals
476 (due to relatedness: 155; missing data or low intensity: 226; gender: 5). We then removed 616,426
477 SNPs that did not pass quality control, leaving a total of 1,767,222 SNPs. We used plink2 to
478 prune the SNPs (options: `-maf 0.01 -indep-pairwise 50 2 0.2`) down to a set of 462,120 SNPs in
479 approximate linkage equilibrium. These SNPs were then used to calculate the first 5 principal
480 components (Figure S15), which we subsequently used to control for population structure in the
481 genome-wide association study. We used the Michigan imputation server with the 1000 Genomes
482 Phase 3 (Version 5) as the reference panel to impute 28.6 million polymorphisms across the 22
483 autosomal chromosomes. This is a web-based service that runs imputation pipelines (phasing is
484 done with Eagle2, imputation with Minimac4). Encrypted results are returned with a one-time
485 password. Of the remaining 3,682 individuals (1,681 cases and 1,615 controls), we had clinical
486 data available for 1,297 cases. We only used the subset of individuals with clinical data available
487 in order for a fair comparison between the weighted and non-weighted genome-wide association
488 studies. We ran subsequent genome wide association studies on all bi-allelic sites with a minor
489 allele frequency $\geq 5\%$ (9,615,446 sites in total) assuming an additive model of association. We
490 used the R function *glm* with a binomial link for all tests of association (genetic data are encoded
491 as the number of reference alleles). The supplementary appendix gives the R code for weighted
492 logistic regression. The point estimates from the weighted model estimated by *glm* are correct
493 but it is necessary to transform the standard errors in order to take into account the reduction in
494 effective sample size (see code).

495 Case-control study in directly typed polymorphisms

496 We fit a categorical (multinomial) logistic regression model to the case-control status as a function
497 of the directly typed polymorphisms (120 after discarding those that are monomorphic in this
498 population, see [27] for additional details). We modelled the severe malaria cases as two separate
499 sub-populations with a latent variable: ‘severe malaria’ versus ‘not severe malaria’, resulting in
500 3 possible labels (controls, ‘severe malaria’, ‘not severe malaria’). The models adjusted for self-
501 reported ethnicity and sex. The model was coded in *stan* [49] using the log-sum-exp trick to
502 marginalise out the likelihood over the latent variables (see code). Normal(0,5) priors were set on

503 all parameters and parameter estimates and standard errors were estimated from the maximum a
504 posteriori value (function *optimizing* in *rstan*).

505 Code availability

506 Code along with a minimal clinical dataset for reproducibility of the diagnostic phenotyping model
507 is available via a github repository: [https://github.com/jwatowatson/Kenyan_phenotypic_](https://github.com/jwatowatson/Kenyan_phenotypic_accuracy)
508 [accuracy](https://github.com/jwatowatson/Kenyan_phenotypic_accuracy).

509 Data availability

510 A curated minimal clinical dataset is currently available alongside the code on the github reposi-
511 tory. This will also be made available at publication via the KEMRI-Wellcome Harvard Data-
512 verse (<https://dataverse.harvard.edu/dataverse/kwtrp>). Whole genome data are available
513 from European Genome-Phenome Archive (dataset accession ID: EGAD00010001742). Requests
514 for access to appropriately anonymized clinical data and directly typed genetic variants for the
515 Kenyan severe malaria cohort can be made by application to the data access committee at the
516 KEMRI-Wellcome Trust Research Programme by e-mail to mmunene@kemri-wellcome.org. The
517 FEAST trial datasets are available from the principal investigator on reasonable request (k.maitland@imperial.ac.uk).
518 Requests for access to appropriately anonymized clinical data from the AQ and AAV Vietnam study
519 and the Asian paediatric cohort can be made via the Mahidol Oxford Tropical Medicine Research
520 Unit data access committee by emailing the corresponding author JAW (jwatowatson@gmail.com)
521 or Rita Chanviriyavuth (rita@tropmedres.ac).

522 Acknowledgements

523 This research was funded by The Wellcome Trust. A CC BY or equivalent licence is applied
524 to the author accepted manuscript arising from this submission, in accordance with the grant's
525 open access conditions. This work was done as part of SMAART (Severe Malaria Africa – A
526 consortium for Research and Trials) funded by a Wellcome Collaborative Award in Science grant
527 (209265/Z/17/Z:) held in part by KM, NPJD and AD. TNW and NJW are senior and principal
528 research fellows respectively funded by the Wellcome Trust (202800/Z/16/Z and 093956/Z/10/C,
529 respectively). ECG acknowledges funding from a core grant to the MRC CTU at UCL from the
530 MRC (MC_UU_12023/26)

531 This study makes use of data generated by MalariaGEN. A full list of the investigators who
532 contributed to the generation of the data is available from www.MalariaGEN.net. Funding for
533 this project was provided by Wellcome Trust (WT077383/Z/05/Z) and the Bill & Melinda Gates
534 Foundation through the Foundation of the National Institutes of Health (566) as part of the Grand
535 Challenges in Global Health Initiative. This study also makes use of data from the FEAST trial.
536 The FEAST trial was supported by a grant (G0801439) from the Medical Research Council, United
537 Kingdom provided through the (MRC) DFID concordat. KM and ECG were supported by this
538 grant.

539 References

- 540 [1] World Health Organization. World malaria report 2020: 20 years of global progress and
541 challenges (2020).
- 542 [2] Carter, R. & Mendis, K. N. Evolutionary and historical aspects of the burden of malaria.
543 *Clinical microbiology reviews* **15**, 564–594 (2002).
- 544 [3] Kariuki, S. N. & Williams, T. N. Human genetics and malaria resistance. *Human Genetics*
545 **139**, 801–811 (2020). URL <https://doi.org/10.1007/s00439-020-02142-6>.
- 546 [4] Teo, Y.-Y., Small, K. S. & Kwiatkowski, D. P. Methodological challenges of genome-wide
547 association analysis in Africa. *Nature Reviews Genetics* **11**, 149–160 (2010).
- 548 [5] Band, G. *et al.* Imputation-based meta-analysis of severe malaria in three African populations.
549 *PLoS Genetics* **9**, e1003509 (2013).

- 550 [6] The Malaria Genomic Epidemiology Network. Reappraisal of known malaria resistance loci
551 in a large multicenter study. *Nature Genetics* **46**, 1197 (2014).
- 552 [7] Band, G. *et al.* Insights into malaria susceptibility using genome-wide data on 17,000 in-
553 dividuals from Africa, Asia and Oceania. *Nature Communications* **10**, 5732 (2019). URL
554 <https://doi.org/10.1038/s41467-019-13480-z>.
- 555 [8] Leffler, E. M. *et al.* Resistance to malaria through structural variation of red blood cell invasion
556 receptors. *Science* **356** (2017).
- 557 [9] White, N. J., Turner, G. D., Day, N. P. & Dondorp, A. M. Lethal malaria: Marchiafava and
558 Bignami were right. *The Journal of Infectious Diseases* **208**, 192–198 (2013).
- 559 [10] Taylor, T. E. *et al.* Differentiating the pathologies of cerebral malaria by postmortem parasite
560 counts. *Nature Medicine* **10**, 143–145 (2004).
- 561 [11] Bejon, P. *et al.* Defining childhood severe falciparum malaria for intervention studies. *PLoS*
562 *Medicine* **4**, e251 (2007).
- 563 [12] Rodriguez-Barraquer, I. *et al.* Quantification of anti-parasite and anti-disease immunity to
564 malaria as a function of age and exposure. *eLife* **7**, e35832 (2018).
- 565 [13] Smith, T., Schellenberg, J. A. & Hayes, R. Attributable fraction estimates and case definitions
566 for malaria in endemic. *Statistics in Medicine* **13**, 2345–2358 (1994).
- 567 [14] WHO. Severe malaria. *Tropical Medicine & International Health* **19**, 7–131
568 (2014). URL https://onlinelibrary.wiley.com/doi/abs/10.1111/tmi.12313_2. https://onlinelibrary.wiley.com/doi/pdf/10.1111/tmi.12313_2.
- 570 [15] Anstey, N. M. & Price, R. N. Improving case definitions for severe malaria. *PLoS Medicine*
571 **4**, e267 (2007).
- 572 [16] Zondervan, K. T. & Cardon, L. R. Designing candidate gene and genome-wide case-control
573 association studies. *Nature Protocols* **2**, 2492–2501 (2007). URL <https://doi.org/10.1038/nprot.2007.366>.
- 575 [17] Nie, L., Zhang, Z., Rubin, D., Chu, J. *et al.* Likelihood reweighting methods to reduce
576 potential bias in noninferiority trials which rely on historical data to make inference. *The*
577 *Annals of Applied Statistics* **7**, 1796–1813 (2013).
- 578 [18] Storey, J. D. A direct approach to false discovery rates. *Journal of the Royal Statistical*
579 *Society: Series B (Statistical Methodology)* **64**, 479–498 (2002).
- 580 [19] Hien, T. T. *et al.* A controlled trial of artemether or quinine in Vietnamese adults with severe
581 falciparum malaria. *New England Journal of Medicine* **335**, 76–83 (1996).
- 582 [20] Phu, N. H. *et al.* Randomized controlled trial of artesunate or artemether in Vietnamese
583 adults with severe falciparum malaria. *Malaria Journal* **9**, 97 (2010).
- 584 [21] Maitland, K. *et al.* Mortality after fluid bolus in African children with severe infection. *New*
585 *England Journal of Medicine* **364**, 2483–2495 (2011).
- 586 [22] Hendriksen, I. C. *et al.* Diagnosing severe falciparum malaria in parasitaemic African children:
587 a prospective evaluation of plasma PfHRP2 measurement. *PLoS Medicine* **9**, e1001297 (2012).
- 588 [23] Reich, D. *et al.* Reduced neutrophil count in people of African descent is due to a regulatory
589 variant in the Duffy antigen receptor for chemokines gene. *PLoS Genetics* **5**, e1000360 (2009).
- 590 [24] Taylor, S. M., Parobek, C. M. & Fairhurst, R. M. Haemoglobinopathies and the clinical epi-
591 demiology of malaria: a systematic review and meta-analysis. *The Lancet Infectious Diseases*
592 **12**, 457–468 (2012).
- 593 [25] Small, D. S. *et al.* Evidence from a natural experiment that malaria parasitemia is pathogenic
594 in retinopathy-negative cerebral malaria. *eLife* **6**, e23699 (2017).

- 595 [26] Uyoga, S. *et al.* The indirect health effects of malaria estimated from health advantages of the
596 sickle cell trait. *Nature Communications* **10**, 856 (2019). URL [https://doi.org/10.1038/
597 s41467-019-08775-0](https://doi.org/10.1038/s41467-019-08775-0).
- 598 [27] Ndila, C. M. *et al.* Human candidate gene polymorphisms and risk of severe malaria in
599 children in Kilifi, Kenya: a case-control association study. *The Lancet Haematology* **5**, e333–
600 e345 (2018).
- 601 [28] Scott, J. A. G. *et al.* Relation between falciparum malaria and bacteraemia in Kenyan children:
602 A population-based, case-control study and a longitudinal study. *The Lancet* **378**, 1316–1323
603 (2011). URL [http://dx.doi.org/10.1016/S0140-6736\(11\)60888-X](http://dx.doi.org/10.1016/S0140-6736(11)60888-X).
- 604 [29] Watson, J. A. *et al.* Collider bias and the apparent protective effect of glucose-6-phosphate
605 dehydrogenase deficiency on cerebral malaria. *eLife* **8**, e43154 (2019).
- 606 [30] Dondorp, A. M., Nosten, F., Stepniewska, K., Day, N. & White, N. Artesunate versus quinine
607 for treatment of severe falciparum malaria: a randomised trial. *The Lancet* **366**, 717–725
608 (2005).
- 609 [31] Dondorp, A. M. *et al.* Artesunate versus quinine in the treatment of severe falciparum malaria
610 in African children (AQUAMAT): an open-label, randomised trial. *The Lancet* **376**, 1647–
611 1657 (2010).
- 612 [32] Clarke, G. M. *et al.* Characterisation of the opposing effects of G6PD deficiency on cerebral
613 malaria and severe malarial anaemia. *eLife* **6**, e15085 (2017).
- 614 [33] Uyoga, S. *et al.* Glucose-6-phosphate dehydrogenase deficiency and the risk of malaria and
615 other diseases in children in Kenya: a case-control and a cohort study. *The Lancet Haematology*
616 **2**, e437–e444 (2015).
- 617 [34] Sadarangani, M. *et al.* An observational study of children with sickle cell disease in Kilifi,
618 Kenya. *British Journal of Haematology* **146**, 675–682 (2009).
- 619 [35] Williams, T. N. & Obaro, S. K. Sickle cell disease and malaria morbidity: a tale with two
620 tails. *Trends in parasitology* **27**, 315–320 (2011).
- 621 [36] Wambua, S. *et al.* The effect of α^+ -thalassaemia on the incidence of malaria and other diseases
622 in children living on the coast of Kenya. *PLoS Medicine* **3**, e158 (2006).
- 623 [37] Leopold, S. J. *et al.* Investigating causal pathways in severe falciparum malaria: A pooled
624 retrospective analysis of clinical studies. *PLoS Medicine* **16** (2019).
- 625 [38] Hanson, J. *et al.* The clinical implications of thrombocytopenia in adults with severe falciparum
626 malaria: a retrospective analysis. *BMC medicine* **13**, 1–9 (2015).
- 627 [39] Leblanc, C. *et al.* Management and prevention of imported malaria in children. update of the
628 french guidelines. *Medecine et maladies infectieuses* **50**, 127–140 (2020).
- 629 [40] Lanneaux, J. *et al.* Retrospective study of imported falciparum malaria in french paediatric
630 intensive care units. *Archives of Disease in Childhood* **101**, 1004–1009 (2016).
- 631 [41] Mornand, P. *et al.* Severe imported malaria in children in France. A national retrospective
632 study from 1996 to 2005. *PLoS ONE* **12**, e0180758 (2017).
- 633 [42] Gérardin, P. *et al.* Outcome of life-threatening malaria in African children requiring endotra-
634 cheal intubation. *Malaria Journal* **6**, 51 (2007).
- 635 [43] Gérardin, P. *et al.* Prognostic value of thrombocytopenia in African children with falciparum
636 malaria. *The American Journal of Tropical Medicine and Hygiene* **66**, 686–691 (2002).
- 637 [44] Williams, T. N. *et al.* Negative epistasis between the malaria-protective effects of α^+ -
638 thalassaemia and the sickle cell trait. *Nature Genetics* **37**, 1253–1257 (2005).
- 639 [45] Opi, D. H. *et al.* Mechanistic studies of the negative epistatic malaria-protective interaction
640 between sickle cell trait and α^+ thalassaemia. *EBioMedicine* **1**, 29–36 (2014).

- 641 [46] Ndila, C. *et al.* Haplotype heterogeneity and low linkage disequilibrium reduce reliable pre-
642 diction of genotypes for the $\alpha^{3.7I}$ form of α -thalassaemia using genome-wide microarray data
643 [version 1; peer review: awaiting peer review]. *Wellcome Open Research* **5** (2020).
- 644 [47] Phu, N. H. *et al.* Concomitant Bacteremia in Adults With Severe Falciparum
645 Malaria. *Clinical Infectious Diseases* (2020). URL [https://doi.org/10.1093/cid/](https://doi.org/10.1093/cid/ciaa191)
646 [ciaa191](https://doi.org/10.1093/cid/ciaa191). Caa191, [https://academic.oup.com/cid/advance-article-pdf/doi/10.1093/](https://academic.oup.com/cid/advance-article-pdf/doi/10.1093/cid/ciaa191/33095946/ciaa191.pdf)
647 [cid/ciaa191/33095946/ciaa191.pdf](https://doi.org/10.1093/cid/ciaa191/33095946/ciaa191.pdf).
- 648 [48] Frühwirth-Schnatter, S. & Malsiner-Walli, G. From here to infinity: sparse finite versus Dirich-
649 let process mixtures in model-based clustering. *Advances in Data Analysis and Classification*
650 **13**, 33–64 (2019). URL <https://doi.org/10.1007/s11634-018-0329-y>.
- 651 [49] Stan Development Team. RStan: the R interface to Stan (2020). URL <http://mc-stan.org/>.
652 R package version 2.21.2.

Severely ill African children (FEAST)

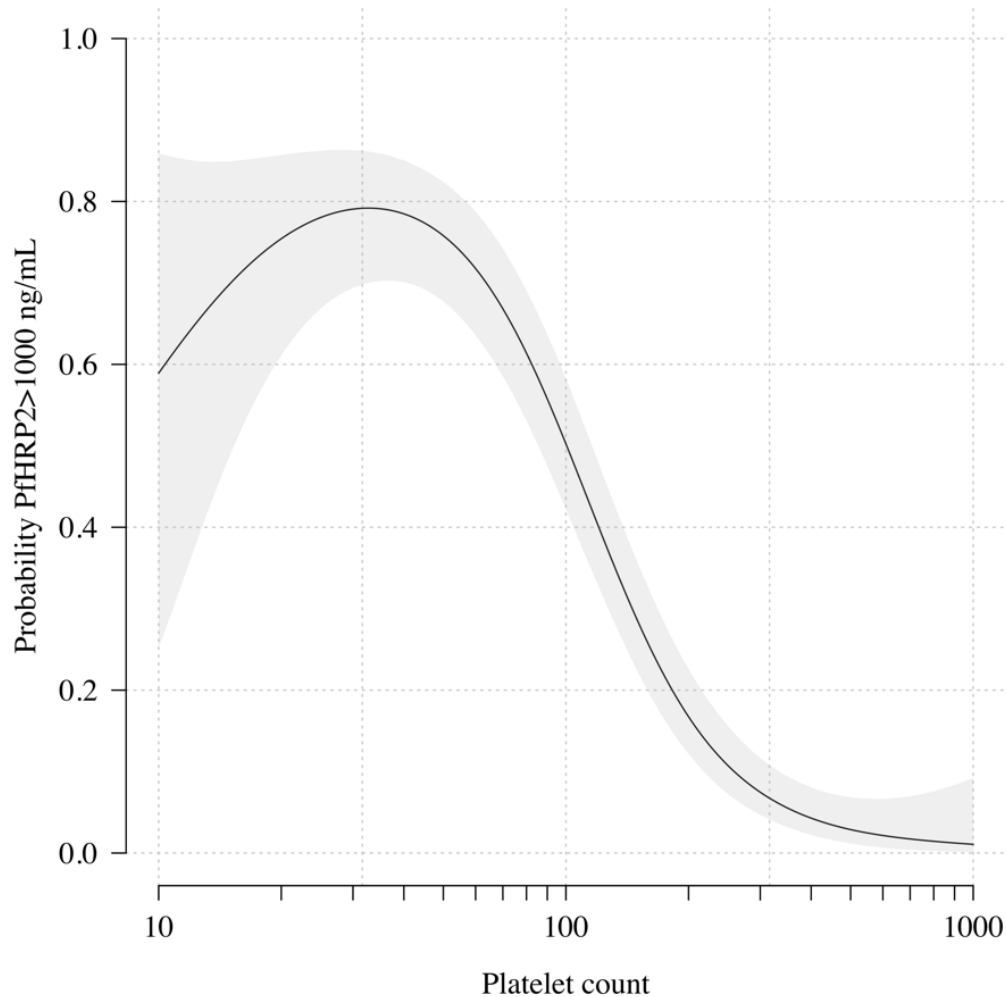


Figure S1: **The relationship between platelet counts and plasma *PfHRP2* in severely ill African children.** The black line (shaded area) shows the estimated probability (95% confidence interval), derived from a generalised additive logistic regression model ($p < 10^{-16}$ for the spline term, fit using the R package *mgcv*), that the plasma *PfHRP2* > 1,000 ng/mL as a function of \log_{10} platelet count. The generalised additive model was fit to data from 566 African children enrolled in the FEAST trial [21] (all the children who had both platelet counts and *PfHRP2* data available). Plasma *PfHRP2* > 1,000 ng/mL is highly discriminatory for severe malaria [22].

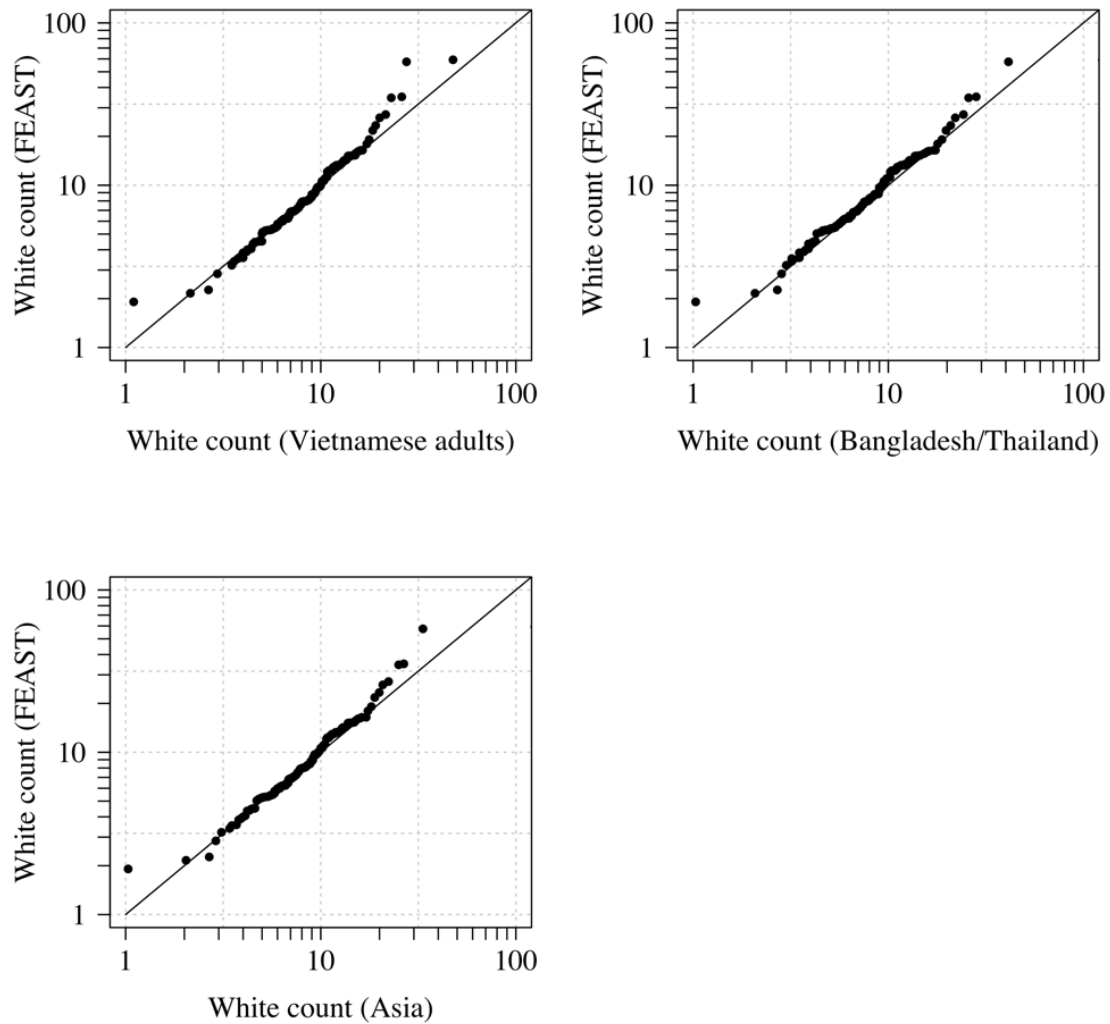


Figure S2: Comparison of the marginal distributions of white blood cell counts between Asian adults and children with severe malaria and African children with severe malaria. FEAST: 121 severely ill Ugandan children with *Pf*HRP2 > 1,000 ng/mL [21]. Vietnamese adults: 930 adults from two large randomised trials in severe malaria [20, 19]. Bangladesh/Thailand: 653 adults and children from observational studies of severe malaria [37].

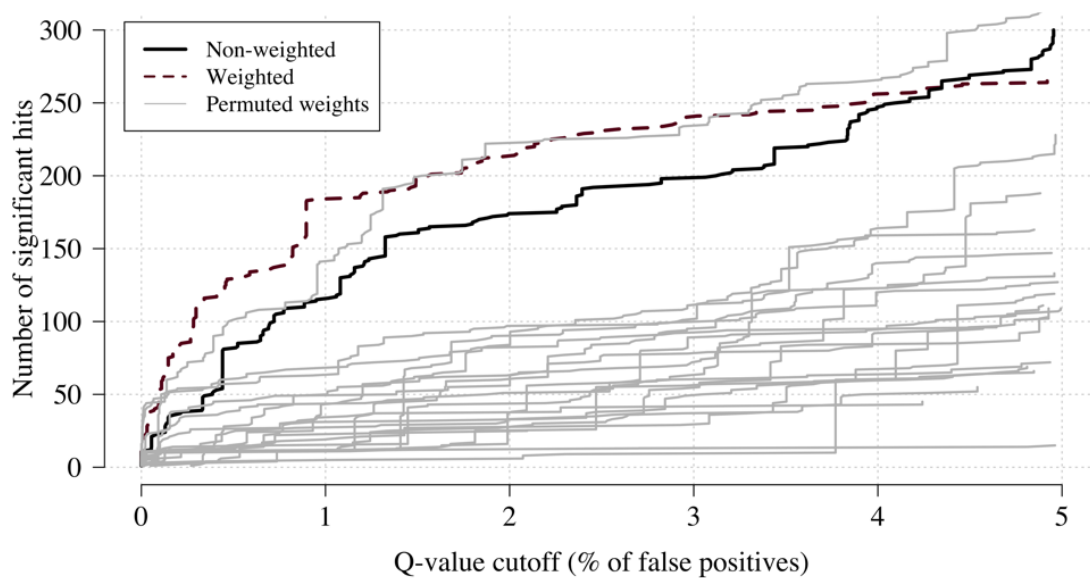


Figure S3: **Effect of permuting the weights in the re-weighted (data-tilting) GWAS.** Here we show the results of 20 random permutations of the weights, applied to the Kenyan case-control GWAS using only chromosomes 4, 9 and 11 (where the top hits are - we limit it to these 3 chromosomes for computational reasons). The random permutations (grey) decrease the number of significant hits compared to the non-weighted (thick black) and the non-permuted re-weighted model (dashed purple).

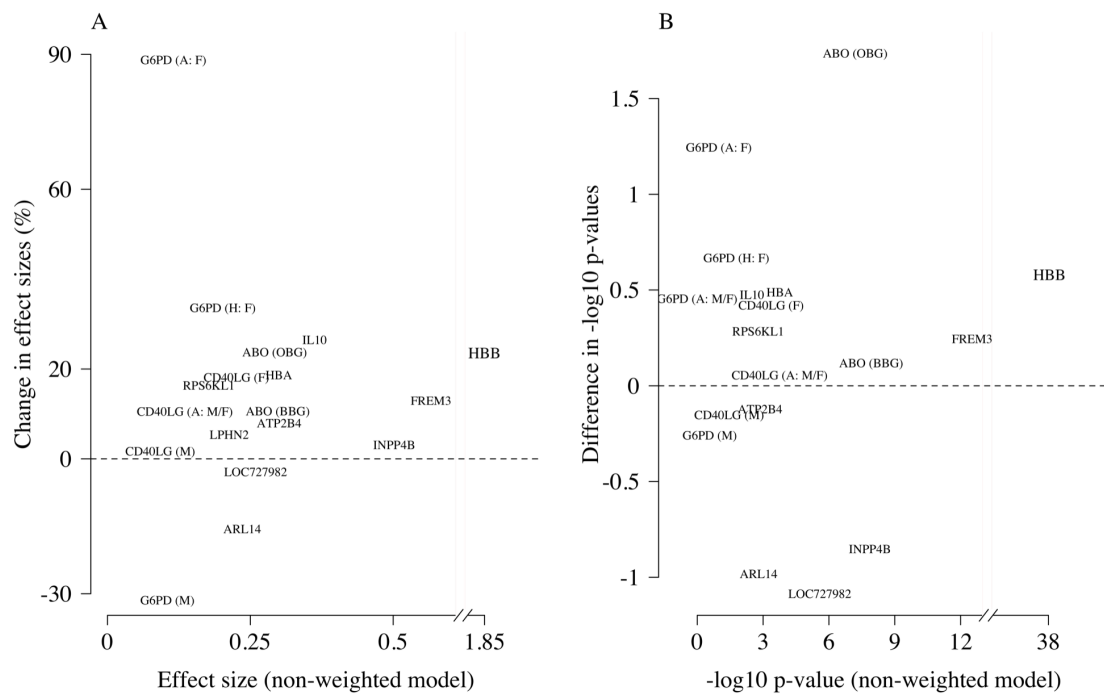


Figure S4: **Comparison of the non-weighted and weighted models of association for directly typed polymorphisms previously reported as associated with severe malaria [27].** Panel A: estimated effect sizes under the non-weighted model versus the difference in effect sizes between the weighted and non-weighted models (absolute effects on the log-odds scale). Differences > 0 imply that the absolute effect size is estimated to be larger under the weighted model. Panel B: $-\log_{10}$ p-values under the non-weighted model versus the differences in $-\log_{10}$ p-values under the weighted and non-weighted models, again differences > 0 represent larger $-\log_{10}$ p-values for the weighted model. Each point is represented by the gene name. In each case we use the model that best fit the data in the original analysis [27]. For the X-linked polymorphisms (*G6PD*, *CD40LG*), multiple models were reported and so the association model is also shown: H (heterozygote); A (additive); M (males only); F (females only); M/F (all).

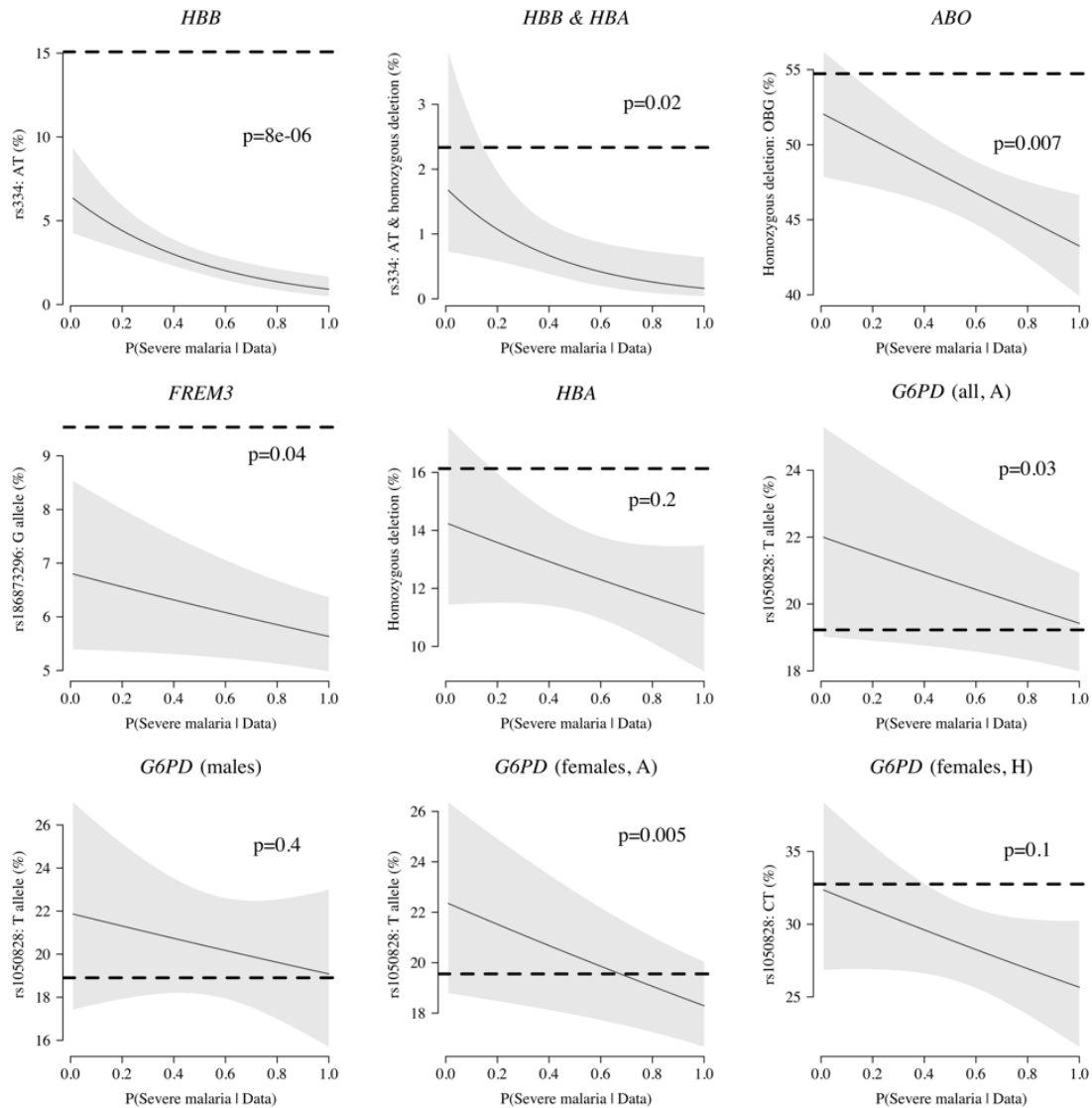


Figure S5: Case-only analysis of five key polymorphisms effecting red cells, reported in [27] under additive, recessive or heterozygote models. The horizontal dashed lines show the estimated frequency in the controls (for additive models this is the frequency of the derived allele, for the heterozygote or recessive models this is the frequency of the genotype thought to confer protection). The line (shaded area) show logistic regression fits with P(Severe malaria | Data) as the predictor (95% confidence interval of the fit). The p-value corresponds to the test that the predictor P(Severe malaria | Data) is not associated with the genotype in the cases only. OBG: O Blood Group

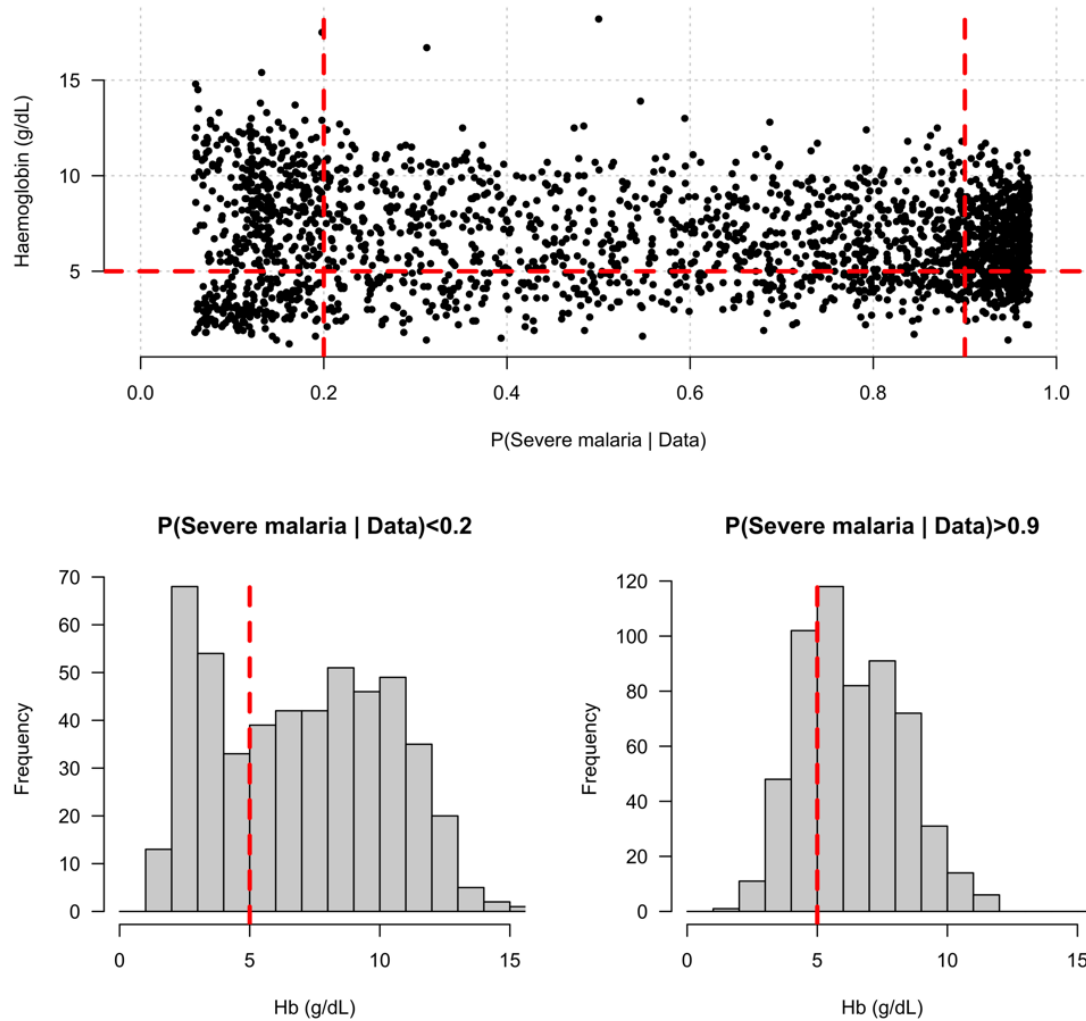


Figure S6: **Distribution of admission haemoglobin concentrations as a function of $P(\text{Severe malaria} \mid \text{Data})$.** Severe anaemia is generally defined as a haemoglobin less than 5 g/dL in African children diagnosed with severe malaria, shown by the horizontal dashed red line in the top panel and the vertical dashed red lines in the bottom panels. The vertical dashed red lines in the top panel show the top and bottom quintiles of the probability distribution (0.9 and 0.2, respectively). Patients in the bottom quintile of the probability distribution had a markedly bi-modal distribution in haemoglobin concentrations with a substantial proportion meeting the severe anaemia criterion and a substantial proportion with relatively high haemoglobin concentrations (> 10 g/dL), suggesting two patients subgroups. Patients in the top quintile had a uni-modal distribution of haemoglobin.

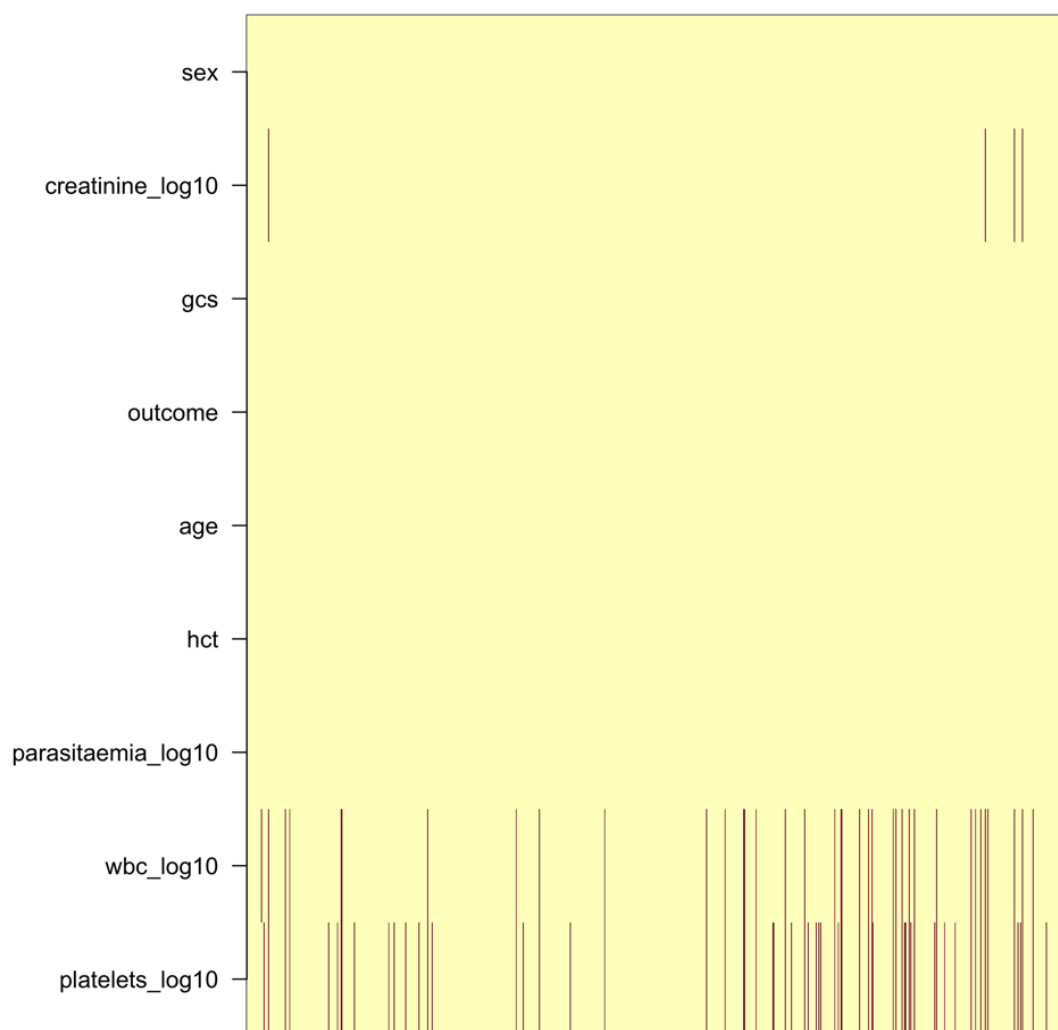


Figure S7: **Pattern of missing clinical data in the 930 Vietnamese adults.** These data pool the AQ Vietnam severe malaria study [19] and the AAV severe malaria study [20] (red: missing; yellow: recorded).

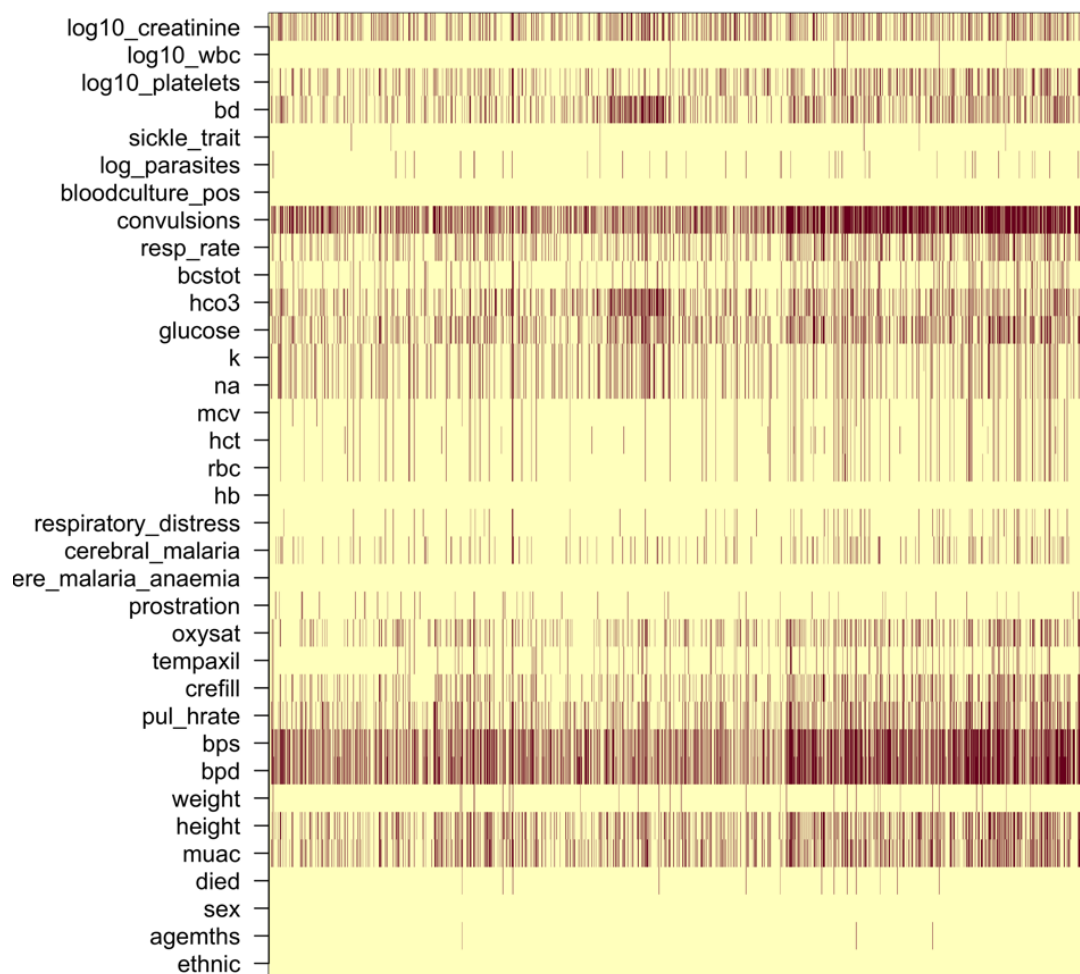


Figure S8: **Missing clinical data in the 2,220 Kenyan children diagnosed with severe malaria** . (red: missing; yellow: recorded).

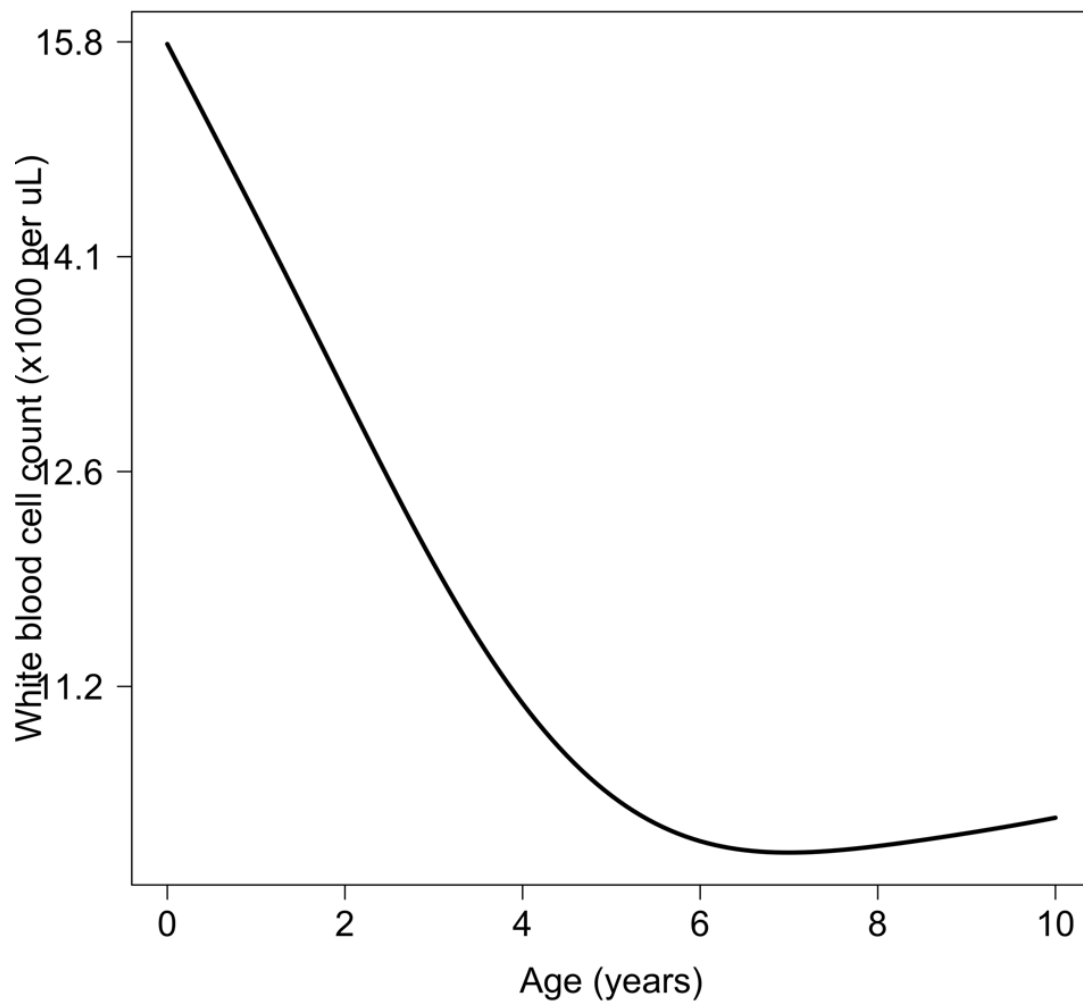


Figure S9: **Relationship between age and mean white count (modelled on the \log_{10} scale)**. This is estimated from 858 children in the FEAST trial who had white counts available using an additive linear model ($p = 10^{-8}$ for the smooth spline term). We used this model to adjust observed \log_{10} white counts in all children less than 5 years of age in the training and testing datasets.

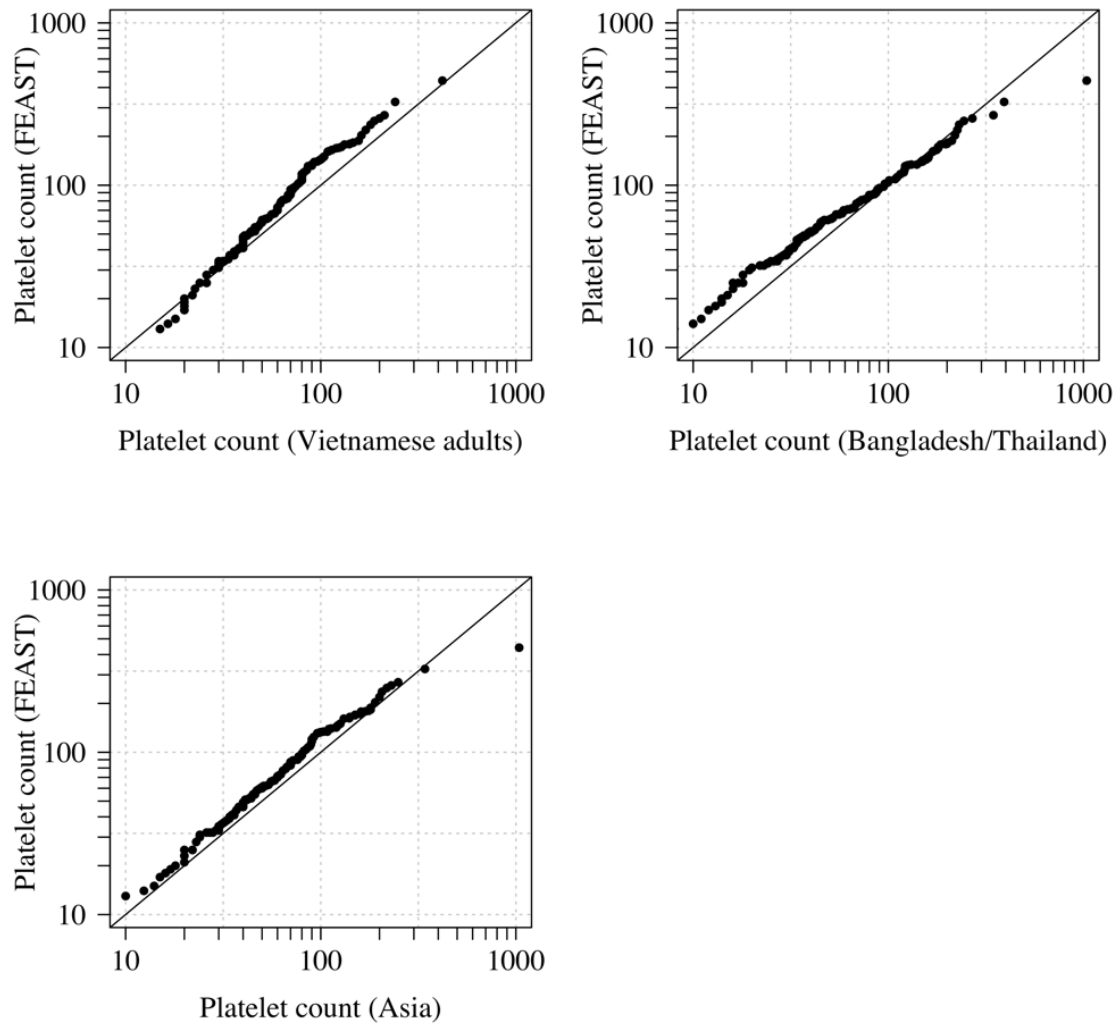


Figure S10: Comparison of the marginal distributions of platelet counts between Asian adults and children with severe malaria and African children with severe malaria. FEAST: 121 severely ill Ugandan children with *PfHRP2* > 1,000 ng/mL [21]. Vietnamese adults: 930 adults from two large randomised trials in severe malaria [20, 19]. Bangladesh/Thailand: 653 adults and children from observational studies of severe malaria [37].

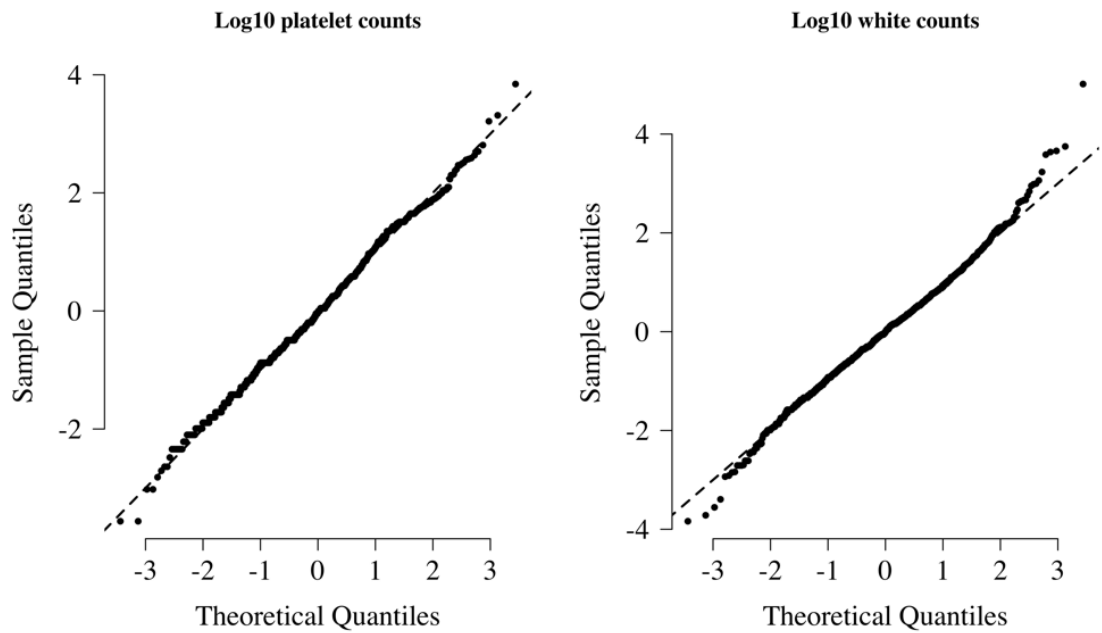


Figure S11: Normal-quantile plots for platelet counts and white blood cell counts in the training data. Both were standardised to have mean 0 and standard deviation of 1 on the \log_{10} scale. The diagonal lines shows the identity line.

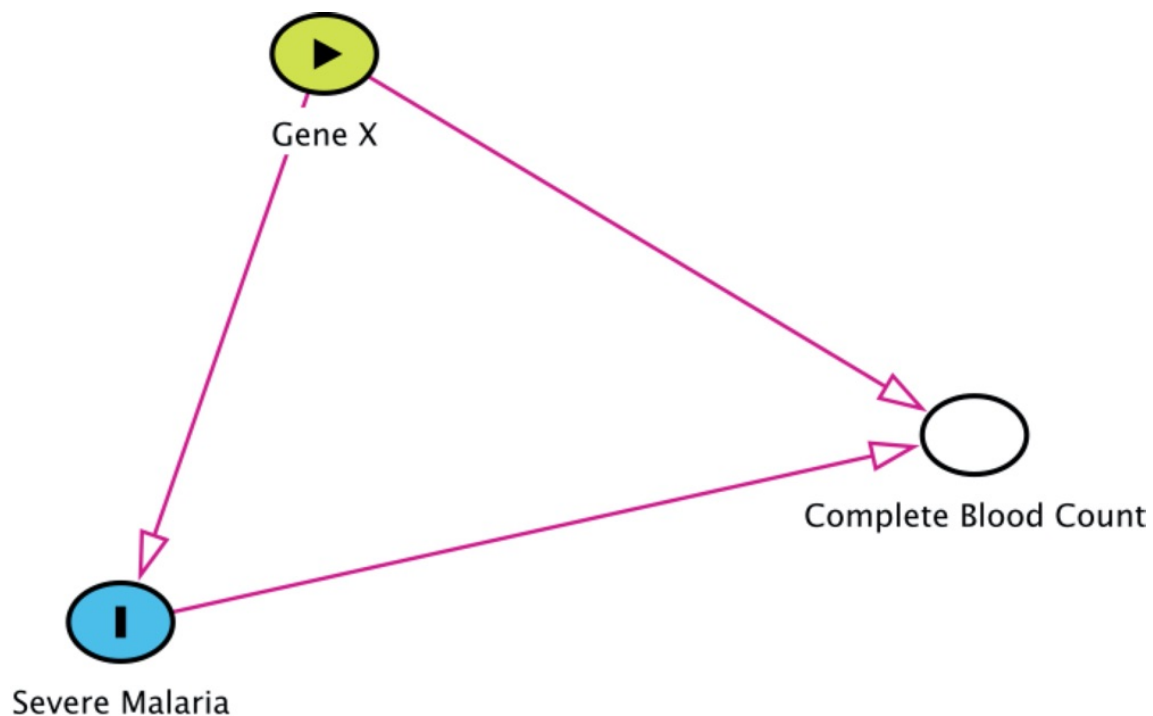


Figure S12: Collider bias in the diagnostic model of severe malaria based on complete blood count data. *HBB* in its homozygous S form (HbSS, <1% prevalence in this Kenyan population) is a rare example of how this can occur. Children with HbSS have white counts above 2-3 times higher than the normal population and slightly lower platelet counts [34]. Under the probabilistic model, all 11 children with HbSS were classified as having a low probability of severe malaria, based on their high white counts (mean 40,000 per μL). These probabilities cannot be taken at face value and it remains an unanswered question whether children with HbSS are more or less susceptible than their wild-type counterparts [35]

Sickle cell anaemia

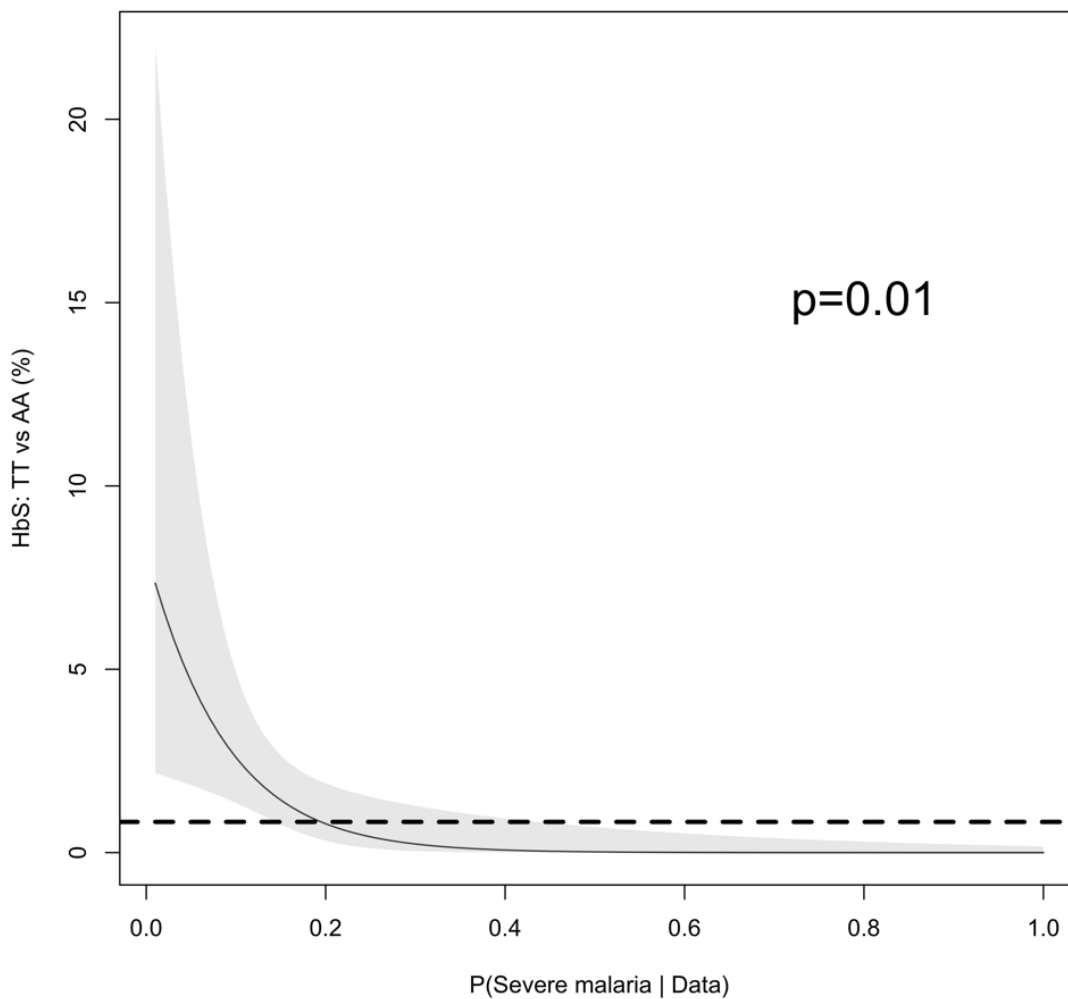


Figure S13: **The relationship between HbSS and the estimated probabilities of severe malaria under the diagnostic model.** There were 11 children with HbSS and they all had low probabilities of severe malaria but this is biased as these children have chronic inflammation with white counts 2-3 higher than the general population [34] (see Figure S12 for the causal diagram showing collider bias).

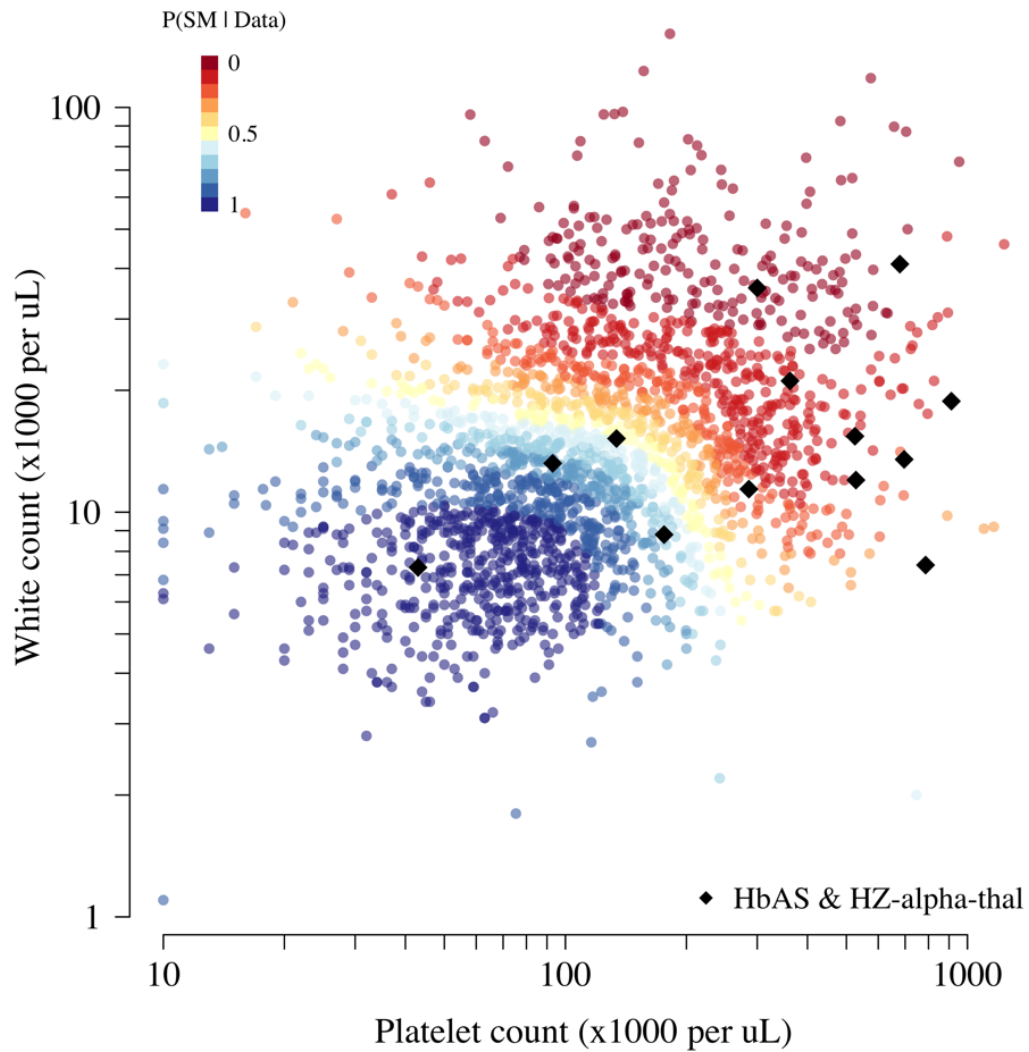


Figure S14: Scatter plots of platelet counts versus white blood cell counts for the Kenyan cohort, showing the 13 individuals with the double mutation HbAS & homozygous α^+ -thalassaemia as large black diamonds (HZ-alpha-thal). The red-yellow-blue colour scheme is proportional to the $P(\text{Severe malaria} \mid \text{Data})$ as given by the legend in the top left corner.

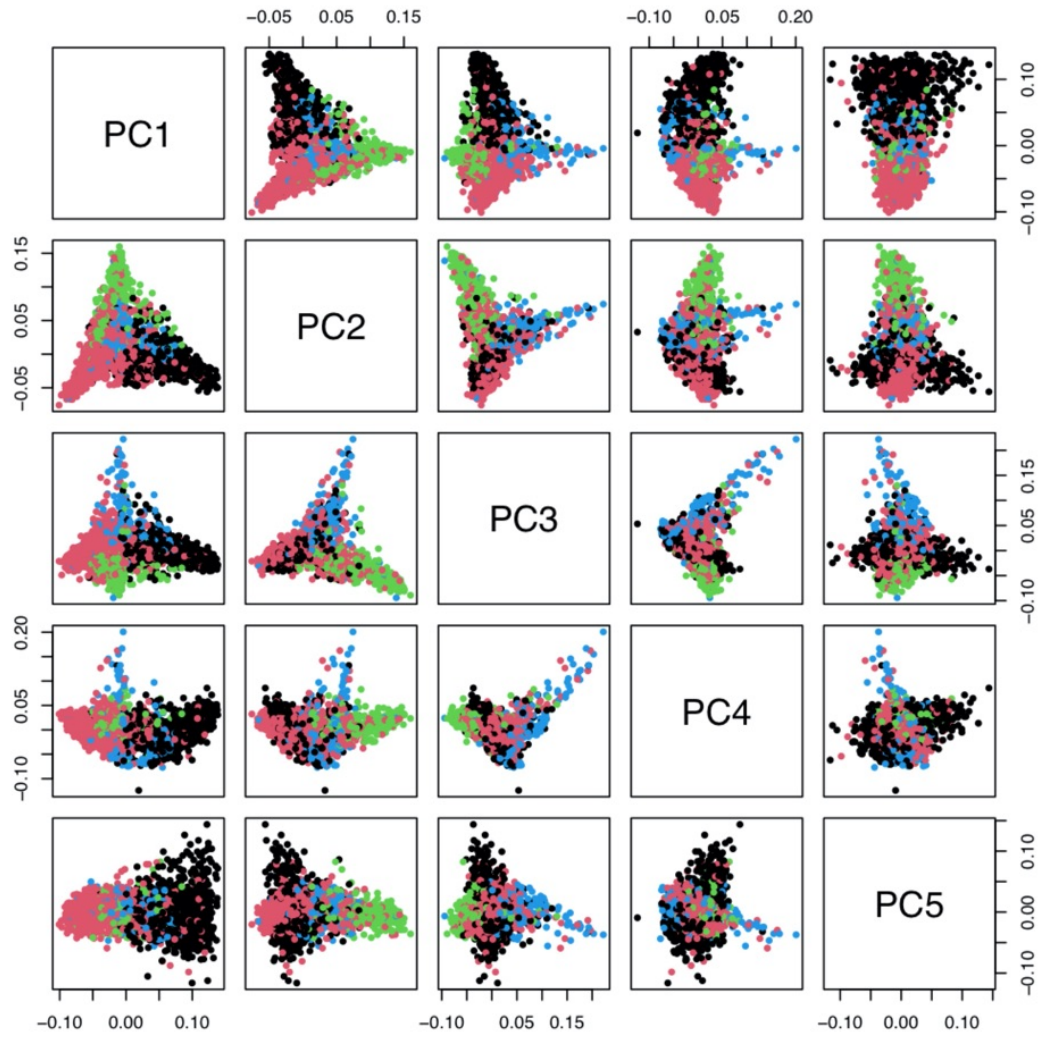


Figure S15: Principal components analysis of 1,666 Kenyan cases and 1,606 population controls. The colours show the main self-reported ethnicities (black: Chonyi; red: Giriama; green: Kauma; blue: other). The first 5 principal components were used to stratify for population structure in the GWAS analyses.